PLEISTOCENE HYDROLOGY OF NORTH AMERICA: THE ROLE OF ICE SHEETS IN REORGANIZING GROUNDWATER FLOW SYSTEMS

Mark Person,[1] Jennifer McIntosh,[2] Victor Bense,[3] and V. H. Remenda[4]

Received 20 June 2006; revised 30 September 2006; accepted 12 December 2006; published 21 September 2007.

[1] While the geomorphic consequences of Pleistocene megafloods have been known for some time, it has been only in the past 2 decades that hydrogeologists and glaciologists alike have begun to appreciate the important impact that ice sheet–aquifer interactions have had in controlling subsurface flow patterns, recharge rates, and the distribution of fresh water in confined aquifer systems across North America. In this paper, we document the numerous lines of geochemical, isotopic, and geomechanical evidence of ice sheet hydrogeology across North America. We also review the mechanical, thermal, and hydrologic processes that control subsurface fluid migration beneath ice sheets. Finite element models of subsurface fluid flow, permafrost formation, and ice sheet loading are presented to investigate the coupled nature of transport processes during glaciation/deglaciation. These indicate that recharge rates as high as 10 times modern values occurred as the Laurentide Ice Sheet overran the margins of sedimentary basins. The effects of ice sheet loading and permafrost formation result in complex transient flow patterns within aquifers and confining units alike. Using geochemical and environmental isotopic data, we estimate that the volume of glacial meltwater emplaced at the margins of sedimentary basins overrun by the Laurentide Ice Sheet totals about 3.7×10^4 km^3, which is about 0.2% of the volume of the Laurentide Ice Sheet. Subglacial infiltration estimates based on continental-scale hydrologic models are even higher (5–10% of meltwater generated). These studies in sum call into question the widely held notion that groundwater flow patterns within confined aquifer systems are controlled primarily by the water table configuration during the Pleistocene. Rather, groundwater flow patterns were likely much more complex and transient in nature than has previously been thought. Because Pleistocene recharge rates are believed to be highly variable, these studies have profound implications for water resource managers charged with determining sustainable pumping rates from confined aquifers that host ice sheet meltwater.

Citation: Person, M., J. McIntosh, V. Bense, and V. H. Remenda (2007), Pleistocene hydrology of North America: The role of ice sheets in reorganizing groundwater flow systems, *Rev. Geophys.*, *45*, RG3007, doi:10.1029/2006RG000206.

1. INTRODUCTION

1.1. Overview

[2] The geomorphic consequences of megafloods associated with Pleistocene glaciations have long been suspected, ever since Joseph Pardee published his seminal paper on the rapid draining of glacial Lake Missoula and the formation of the channeled scablands across Washington state, United States [*Pardee*, 1942]. This and more recent work [e.g., *Rains et al.*, 1993; *Baker*, 1997] provide dramatic evidence of how melting of the Laurentide Ice Sheet influenced the surface water hydrology of North America. However, it has only been in the past 2 decades that hydrogeologists have begun to recognize the important role that ice sheet meltwater has played in controlling the subsurface plumbing within sedimentary basins, especially those who's margins and interiors were repeatedly glaciated during the Pleistocene. Increased hydraulic heads beneath temperate ice sheets may have greatly enhanced recharge of dilute groundwaters into confined aquifers, reorganizing regional-scale flow systems and modifying salinity gradients [e.g., *Grasby et al.*, 2000]. Beyond the continental ice sheet margins, permafrost development may have inhibited meteoric recharge and likely promoted deeper, longer-distance circulation of glacial meltwater. In this paper, we review geochemical, isotopic, hydrologic, and geomechanical evidence for the invasion of Laurentide Ice Sheet meltwaters into underlying aquifer systems and present the compelling case that continental glaciation has profoundly altered basinal-scale groundwater flow in the stable interior of North America repeatedly during the past 2 million years.

[1]Department of Geology, Indiana University, Bloomington, Indiana, USA.
[2]Department of Hydrology and Water Resources, University of Arizona, Tucson, Arizona, USA.
[3]School of Environmental Sciences, University of East Anglia, Norwich, UK.
[4]Department of Geological Sciences and Geological Engineering, Queen's University, Kingston, Ontario, Canada.

8755-1209/07/2006RG000206$15.00
Paper number 2006RG000206

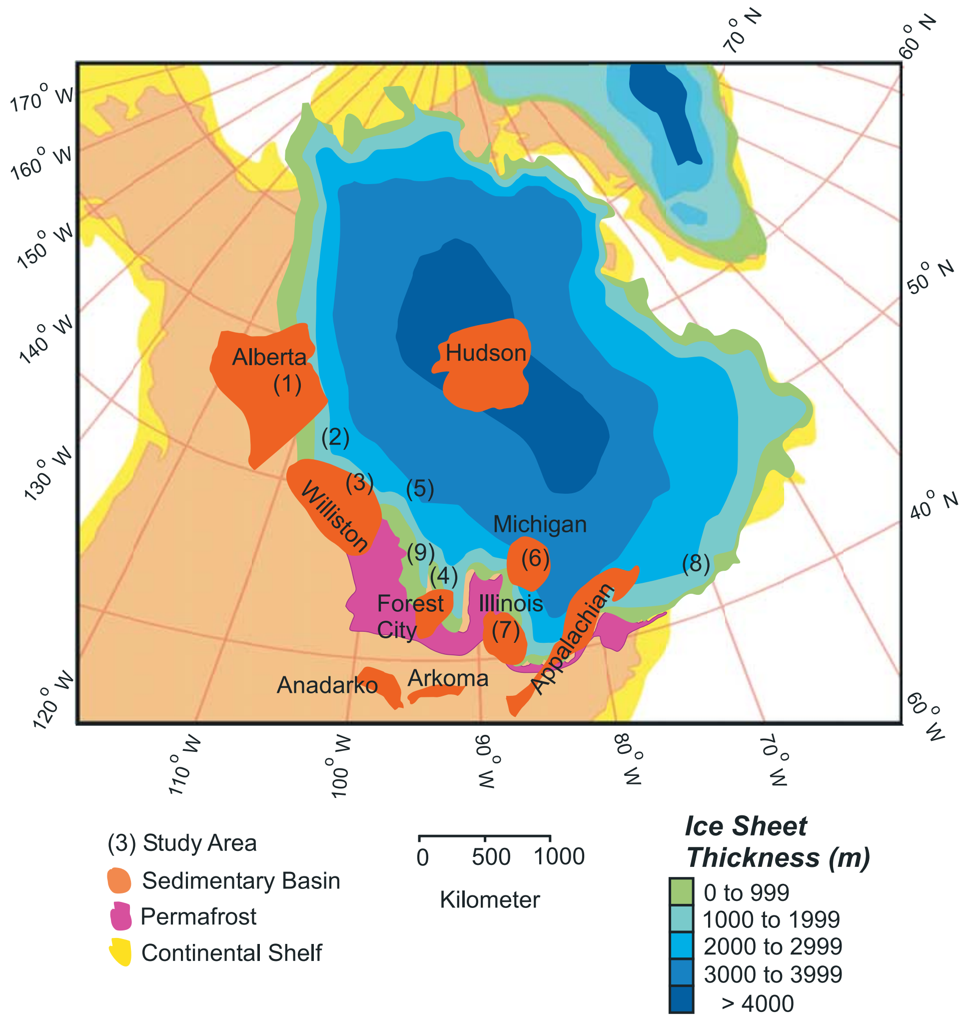

Figure 1. Location of sedimentary basins, thickness of Laurentide Ice Sheet, and southern extent of permafrost across North America. The numbers in parentheses indicate the locations of study sites where researchers have identified ice sheet–aquifer and/or confining unit interactions: 1, *Bekele et al.* [2003]; 2, *Hendry and Wassenaar* [1999]; 3, *Grasby et al.* [2000], *Grasby and Betcher* [2002], and *Grasby and Chen* [2005]; 4, *Siegel and Mandle* [1984]; 5, *Remenda et al.* [1994]; 6, *Martini et al.* [1996], *Hoaglund et al.* [2004], *Ma et al.* [2004], and *McIntosh and Walter* [2006]; 7, *Stueber and Walter* [1994], *Breemer et al.* [2002], and *McIntosh et al.* [2002]; 8, *Oldale and O'Hara* [1984] and *Person et al.* [2003]; and 9, *Mooers* [1990]. Figure 1 is adapted from *Denton and Hughes* [1981], *Pewe* [1983], *Bethke and Marshak* [1990], reprinted with permission from the *Annual Review of Earth and Planetary Sciences*, copyright 1990 by Annual Reviews (http://www.annualreviews.org), and *Stott and Aitken* [1993].

Several sites have been identified (numbers within parentheses in Figure 1), which contain evidence of ice sheet–groundwater interactions that will be discussed in detail in sections 3–5.

[3] The study of the origin of ice sheet–derived groundwater is of relevance to the hydrologic community for a number of reasons. Because ice sheet meltwaters were likely recharged at substantially higher rates than at present, understanding their occurrence and distribution in the subsurface is important to water resource managers charged with determining safe aquifer yields of heavily utilized confined aquifer systems (e.g., Mount Simon Aquifer in SE Minnesota and Chicago). In addition, ice sheet meltwater is generally of excellent quality and because of its age (typically 14–21 ka) it is not tainted by groundwater contamination associated with the postindustrial revolution [*Edmunds*, 2001]. Biogenic gas resources currently being exploited by the petroleum industry are now recognized to be associated with ice sheet meltwater plumes within the Michigan and Illinois basins [*Martini et al.*, 1996, 1998; *McIntosh et al.*, 2002, 2004]. The lowering of sea level associated with the buildup of continental ice exposed large portions of the continental shelf to meteoric recharge [*Groen et al.*, 2000; *Person et al.*, 2003]. Sea level lowstands and continental shelf sub–ice sheet recharge help to explain well-documented occurrences of freshwater to brackish water plumes up to 100 km off the coast of New England [*Kohout et al.*, 1977; *Person et al.*, 2003] and more

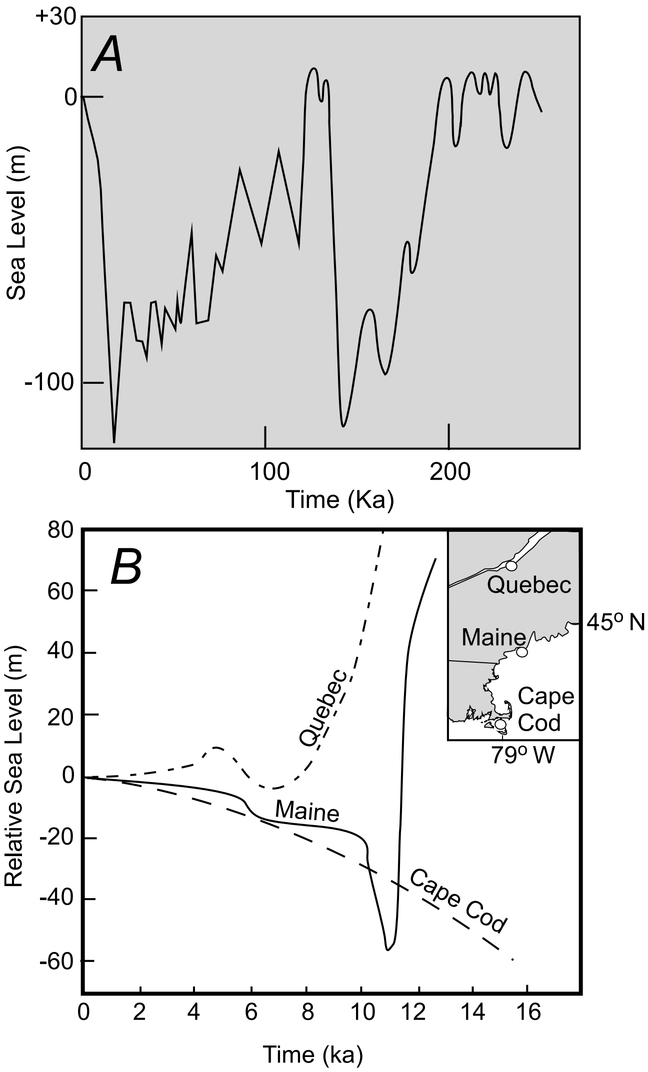

Figure 2. Late Pleistocene (a) eustatic and (b) isostatic sea level fluctuations. Isostatic sea level fluctuations are due to the formation of a moat and forebulge induced by ice sheet loading, lithosphere flexure, and mantle flow on the Atlantic continental shelf in Nova Scotia and New England [after *Barnhardt et al.*, 1995]. The eustatic sea level fluctuations are from *Otvos* [2005], reprinted with permission from Elsevier.

typically 20–40 km offshore [*Meisler et al.*, 1984; *Essaid*, 1990; *Voss and Andersson*, 1993]. With dwindling supplies of potable groundwater in coastal areas, offshore freshwater plumes associated with Pleistocene sea level lowstands and ice sheet meltwaters may represent important freshwater resources (or brackish water for desalinization facilities) in arid regions of the world such as Saudi Arabia as well as near large urban centers in more temperate climates. The importance of Pleistocene recharge has been recognized for some time by the European community who sponsored the Palaeo Waters (PALEAUX) project during the 1990s. This initiative investigated the role of the Fennoscandian ice sheet in controlling the distribution of fresh groundwater in coastal aquifer systems across Europe. The PALEAUX project brought together hydrologists from the United Kingdom, Estonia, Denmark, France, Spain, Portugal, and Switzerland and resulted in the Geological Society of London special publication [*Edmunds*, 2001] that inventoried Pleistocene freshwater resources across Europe. Our paper is an attempt to summarize related studies of Pleistocene hydrology associated with the Laurentide Ice Sheet in North America.

1.2. Ice Sheet Topography, Routing of Glacial Meltwaters, Sea Level Change, and Permafrost

[4] During the last 2 million years, ice sheets have dominated the landscape of North America covering much of the northern United States above a latitude of 48°N and virtually all of Canada (Figure 1). Much of this ice-covered region was in the relatively low-lying interior of the North American craton. Ice sheet thicknesses across North America varied between 0 and 4 km (Figure 1). Numerical models and geologic reconstructions of ice sheet thicknesses and lithosphere deflection reveal that a large mound of ice accumulated over the Hudson Bay region of Canada as a result of Pleistocene climatic patterns [*Peltier*, 1996b; *Marshall et al.*, 2002]. The topography of the ice sheets did not closely mimic that of the continental land surface. Ice sheets advanced and retreated multiple times during the last 2 million years [*Shackleton*, 1987] with periods of about 40 ka and 100 ka. In addition, only about 20% of the Pleistocene period could be characterized by relatively warm, ice-free conditions in Canada and the United States. Thus ice sheet–aquifer interactions may have been the rule rather than the exception across much on North America during the last 2 million years.

[5] Precise age dating of marine corals from Barbados [*Bard et al.*, 1990a, 1990b] as well as sedimentological [*Haq et al.*, 1987] and marine oxygen isotope [*Milliman and Emery*, 1968; *Raymo et al.*, 1997; *Shackleton and Opdyke*, 1973; *Shackleton*, 1987] records indicates that the waxing and waning of ice sheets also resulted in sea level fluctuations, by over 120 m, exposing large areas of the continental shelf to meteoric recharge and increasing the hydraulic head gradient between the continents and the oceans. Pleistocene sea level fluctuations mimicked a sawtooth pattern (Figure 2a), decreasing slowly with the slow growth rate of ice sheets and increasing rapidly with the much higher rate of melting. On the continental shelf in New England, sea level fluctuations were complex because of the propagation of a flexural bulge (Figure 2b) [*Oldale*, 1988; *Barnhardt et al.*, 1995; *Uchupi et al.*, 1996; *Oldale et al.*, 1993]. The formation of large depressions or moats created by the rapidly retreating ice sheet on the continental shelf in the latest Pleistocene submerged much of the southern Maine coastline today (as evidenced by the glaciomarine Presumscott formation [*Oldale and Coleman*, 1990]). The migrating flexural forebulge had an amplitude of about 20 m as it moved across Quebec and southern Maine at a rate of about 9 m/yr during the late Pleistocene [*Barnhardt et al.*, 1995] (Figure 2b).

[6] As the ice sheets grew, they stored large volumes of fresh waters on the continent. The Laurentide Ice Sheet

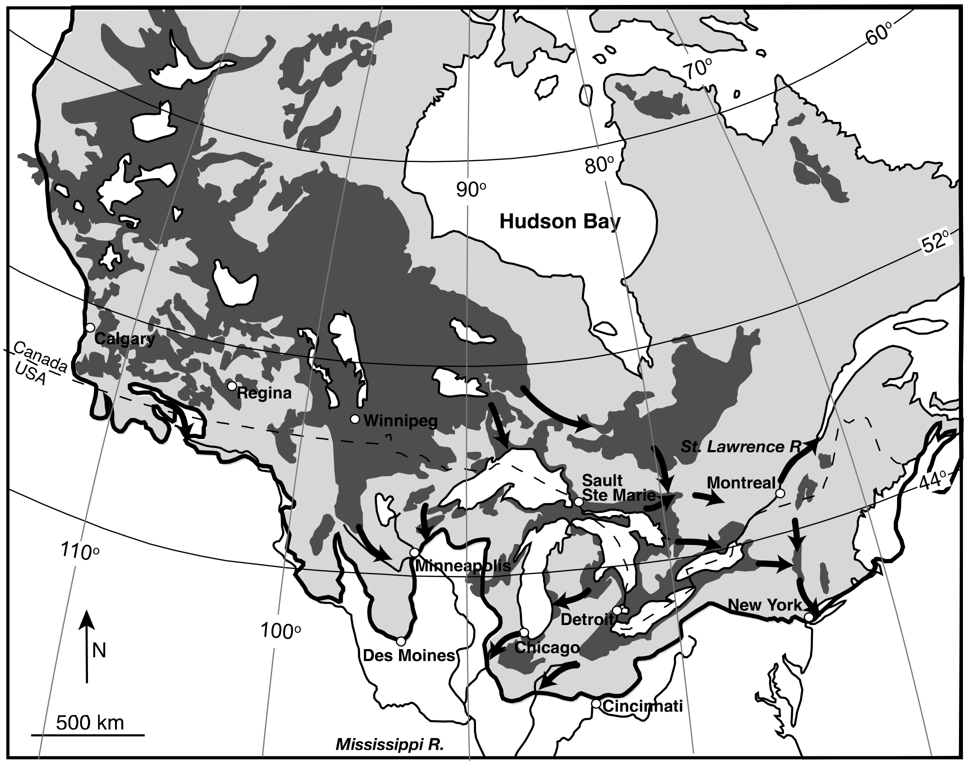

Figure 3. Routing of glacial runoff into the Mississippi and St. Lawrence River drainages (arrows indicate direction of surface water discharge), following the Last Glacial Maximum. Areas covered by lacustrine glacial deposits are shown with dark shading. The extent of the continental ice sheet is outlined with the thick black line and light shaded coverage. Figure 3 is modified from *Teller and Kehew* [1994]. Reprinted with permission from Elsevier.

likely contained greater than 20×10^6 km^3 of water [*Teller*, 1990]. As the ice sheets melted, fresh water was discharged into major drainage systems and transported to the Atlantic Ocean (Figure 3). Riverine fluxes were 2 to 3 times greater than modern surficial runoff [*Marshall and Clarke*, 1999]. Introduction of these cold, dilute waters to the oceans may have drastically changed thermohaline circulation and thus global climate by shutting down Gulf Stream circulation [*Licciardi et al.*, 1999]. As noted above, geomorphic consequences of this catastrophic freshwater discharge from glacial lakes is well documented for glacial lakes Missoula and Agassiz. What is not known is how much of this impounded fresh water infiltrated into subsurface aquifers. No systematic estimates have been made to date at the continental scale of how much of this meltwater recharged subsurface aquifer systems. Subsurface recharge is controlled by the permeability of the sedimentary units overrun by the ice sheet as well as the presence/absence of permafrost. The southern margin of the Laurentide Ice Sheet was likely covered by permafrost during the Last Glacial Maximum (LGM) [*Cutler et al.*, 2000] (purple areas in Figure 1). There is little evidence of permafrost, however, in the Great Lakes basins, likely because these low-lying areas were covered by proglacial lakes [*Larson et al.*, 2003].

[7] Some glacial features across North America suggest a significant portion of glacial meltwaters infiltrated into bedrock aquifers, beneath wet-based ice sheets (i.e., liquid water present at base of ice sheet, temperature at base of ice sheet is above freezing point). The distribution of gravels and tills and landforms in south central Michigan, for example, point to subglacial flooding during retreat of the Saginaw lobe of the Laurentide Ice Sheet [*Fisher and Taylor*, 2002; *Fisher et al.*, 2003]. Esker systems in glaciated regions of Canada are primarily located in areas underlain by crystalline bedrock [*Clark and Walder*, 1994], where the low hydraulic conductivity of the Canadian Shield likely prevented infiltration of meltwaters into underlying bedrock aquifers. In contrast, regions underlain by more permeable Paleozoic carbonate and sandstone aquifers lack extensive esker systems, indicating subglacial waters were able to discharge into basinal flow systems [*Grasby and Chen*, 2005]. This suggests that sub–ice sheet pressure reduction associated with aquifer drainage changed the composition of tills.

1.3. Pleistocene Mean Annual Temperature

[8] The Laurentide Ice Sheet is believed to have changed the position of the North America jet stream modifying climatic conditions in ice-free areas [*COHMAP Members*, 1988]. Because evapotranspiration rates (and hence aquifer recharge) across North America are influenced by mean annual surface air temperatures [*Dingman*, 1994], it is likely that the Laurentide Ice Sheet influenced recharge rates far beyond its terminus [e.g., *Zhu et al.*, 1998]. Multiple studies of the stable isotope and noble gas composition of confined groundwater systems in North America have shown that the

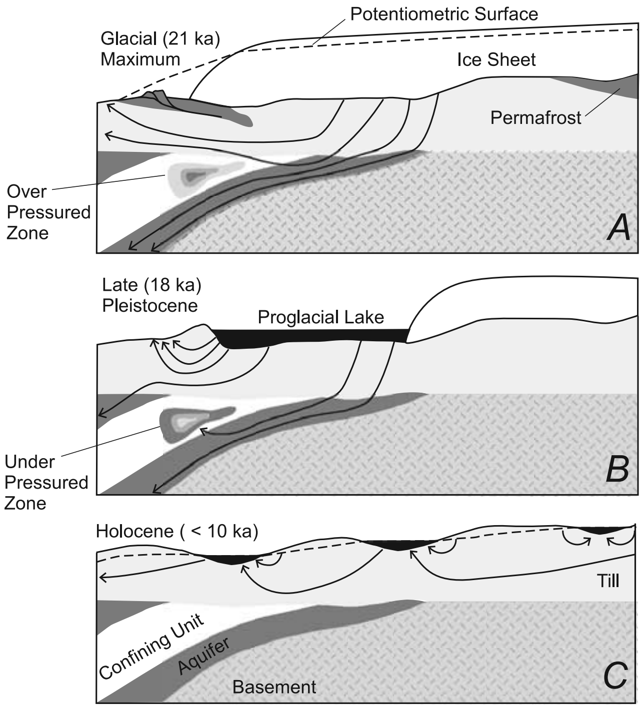

Figure 4. Conceptual model of changes in groundwater hydrogeology across midcontinent regions of North America during (a) Wisconsinan glacial maximum, (b) late Pleistocene ice sheet retreat, and (c) Holocene-Recent. Groundwater flow directions are indicated by the arrows. Ice sheet loading and unloading could have led to the development of anomalously high (Figure 4a) and low (Figure 4b) pressures within low-permeability confining units. During the last glacial maximum, high hydraulic heads beneath the ice sheet (approximately 90% the height of the ice sheet) drove groundwater past the ice sheet terminus into confined aquifers, as well as beyond the permafrost zone into shallower, permeable sediments. Recharge into confined aquifers could have also been induced by seepage through lacustrine sediments. Since the Holocene, local, shallow flow systems dominate. The water table geometry is a subdued replica of the land surface. Figure 4 is modified from *Boulton et al.* [1995], *Toth* [1962], and *Winter* [2001].

mean annual temperature during the Pleistocene was approximately 5° to 9°C cooler than the Holocene. This has been confirmed by pollen-based estimates of late Pleistocene temperatures [*Webb et al.*, 1998]. The noble gas content of groundwater formed by direct recharge of precipitation is largely determined by the dissolution equilibrium with the atmosphere, which is a function of the temperature at the water table. The temperature dependence has been widely used to infer noble gas–derived recharge temperatures in paleoclimate applications for the tropics [e.g., *Stute et al.*, 1995a; *Weyhenmeyer et al.*, 2000] and in midlatitudes [e.g., *Stute et al.*, 1995b; *Aeschbach-Hertig et al.*, 2002] on different continents. The concentrations of these gases in groundwater are determined mainly by pressure-dependent solubility equilibrium with air in the unsaturated zone during infiltration. Noble gases dissolved in confined groundwaters in the Carrizo Aquifer in Texas show the mean annual temperature during the LGM was about 5°C cooler than present [*Stute et al.*, 1992]. Noble gas results from groundwaters in the San Juan Basin, northwestern New Mexico, show the same temperature trend (5.5°C less than modern) [*Stute et al.*, 1995b], indicating a uniform cooling of the southwestern United States, during the LGM. Mean annual temperatures may have been even colder closer to the ice margin. Confined groundwaters in the Aquia Aquifer (Maryland), proximal to the Laurentide Ice Sheet margin at the LGM, have noble gas temperatures 9°C cooler than modern conditions [*Aeschbach-Hertig et al.*, 2002]. *Ma et al.* [2004] report noble gas temperatures of ∼1°C for two groundwater samples in the Marshall sandstone aquifer (Michigan) that are ∼17,400 years old. The near-freezing recharge temperature and apparent age of these waters indicate they were recharged beneath the retreating ice sheet. On the basis of $\delta^{18}O$ values of pore waters from thick Lake Agassiz clays, *Remenda et al.* [1994] calculated a mean annual air temperature of about −16°C for about 48° to 50°N latitude. Interestingly, along the east coast of the United States in the mid-Atlantic regions to the south of the Laurentide Ice Sheet, there is little evidence of temperature-induced shifts in the oxygen isotopic values of late Pleistocene-age precipitation that should be observed as a result of these inferred lower temperatures [*Aeschbach-Hertig et al.*, 2002]. This may be due to changes in trajectories of continental air mass associated with deflection of the jet stream caused by the presence of the Laurentide Ice Sheet [*COHMAP Members*, 1988].

1.4. Pleistocene Hydrology

[9] A conceptual model describing changes in subsurface patterns resulting from ice sheet–aquifer interactions is presented in Figure 4. Since the beginning of the Holocene, continental aquifer systems have been driven by gradients in water table topography modified by the effects of geology [*Tóth*, 1962; *Freeze and Witherspoon*, 1968] (Figure 4c). Deep groundwater flow systems within sedimentary basins are also influenced by the presence of basinal brines [*Hanor*, 1987a; *Garven and Freeze*, 1984; *Appold and Garven*, 1999]. In the glaciated midwestern United States most present-day groundwater flow is restricted to shallow aquifers. Local variations in water table elevation controls groundwater flow directions as first proposed by *Tóth* [1962] and refined by *Freeze and Witherspoon* [1968]. However, there is growing evidence that ice sheets have significantly modified this paradigm of the plumbing of continental aquifer systems (Figures 4a and 4b). For temperate ice sheets the potentiometric heads beneath glaciers are elevated [*Boulton and Zatsepin*, 2006] and can approach 90% of the height of the ice sheet [*Engelhard and Kamb*, 1997]. There is compelling evidence that the magnitude of recharge into confined aquifer systems overrun by the Laurentide Ice Sheet was much greater than present-day conditions [*Grasby et al.*, 2000; *Person et al.*, 2003; *McIntosh and Walter*, 2005]. In areas where the base of

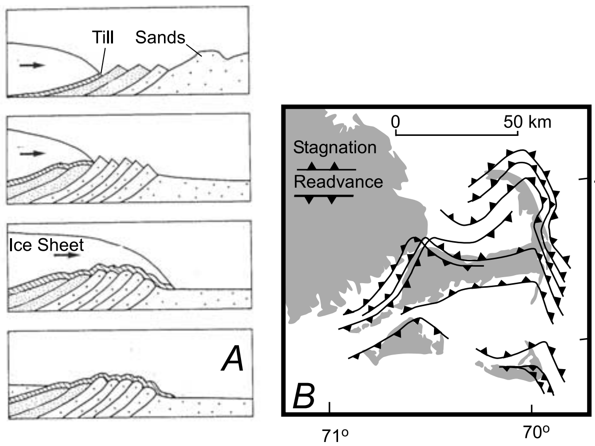

Figure 5. (a) Conceptual model of formation of thrust sheets in undeformed, frozen sediments beneath the terminus of the Laurentide Ice Sheet on the Atlantic continental shelf, New England. (b) Surface expressions of ice sheet thrust structures on Cape Cod, Martha's Vineyard, and Nantucket Islands. Figure 5 is modified from *Oldale and O'Hara* [1984].

the ice sheet is frozen, or in permafrost zones beyond the toe of the ice sheet, there is evidence that recharge was negligible [*Edmunds*, 2001]. Thus, during much of the Pleistocene, the elevation of the ice sheet rather than the land surface topography controlled groundwater flow directions in underlying sedimentary aquifers (Figure 4a). Confining units overrun by the ice sheet would have developed anomalously high fluid pressures and low effective stress, which could have led to deformation features [*Mooers*, 1990; *Stewart et al.*, 2000] (Figure 4a). Mechanical loading would have been greatest at the toe of the ice sheet causing anomalously high fluid pressures in tight confining units (Figures 4a and 4b). This could have caused hydrofracturing of shale units and may help to explain the occurrence of fresh water in confining units at the margins of the Illinois and Michigan basins [*McIntosh et al.*, 2002]. As the Laurentide Ice Sheet retreated during the late Pleistocene (Figure 4b), numerous proglacial lakes formed across the North American craton [*Teller and Kehew*, 1994] and on the Atlantic continental shelf [*Uchupi et al.*, 1996, 2001; *Uchupi and Mulligan*, 2006]. These may have also been an important source of recharge to confined aquifer systems [*Marksamer et al.*, 2007]. Ponded water in proglacial lakes would have attained heads as high as glacial end moraines (as much as 30 m). Focused discharge just beyond the terminus of proglacial lakes helps to explain erosional features near the terminus of the Laurentide Ice Sheet in New England, United States [*Uchupi and Oldale*, 1994]. Because ice sheets retreated much faster than they advanced, ice sheet unloading rates could have been quite high and led to the formation of under-pressure zones within confined aquifers (Figure 4b). *Bekele et al.* [2003] argued for this to explain the occurrence of subhydrostatic heads within thick confining units of the Alberta Basin.

[10] This new paradigm, which represents a tectonic shift in thinking regarding the driving forces on groundwater flow systems within sedimentary basins across North America, emerged from two different lines of evidence. Beginning in the 1980s, hydrogeologists began to recognize anomalous groundwater isotopic patterns in confined bedrock aquifers [*Siegel and Mandle*, 1984], in surficial confining units [*Remenda et al.*, 1994; *Hendry and Wassenaar*, 1999], and more recently in coastal aquifers and deep sedimentary basins [*Grasby et al.*, 2000; *McIntosh et al.*, 2002; *Person et al.*, 2003; *McIntosh and Walter*, 2005; *Grasby and Chen*, 2005]. Growth and decay of ice sheets likely changed the vertical load and fluid pressures in underlying aquifers and confining units [*Stewart et al.*, 2000; *Bekele et al.*, 2003]. Beginning in the 1980s, glaciologists began to appreciate the important role of high excess heads associated with sub–ice sheet–aquifer systems in accounting for unusual geomorphic features near the terminus of ice sheets, including ice-related tectonic features such as thrust structures [*Oldale and O'Hara*, 1984; *Mooers*, 1990] (Figure 5), sand dikes, blowout structures [*Grasby et al.*, 2000; *Christiansen et al.*, 1982], esker systems confined to low-permeability bedrock [*Boulton and Caban*, 1995; *Grasby and Chen*, 2005], and softened zones within overconsolidated shales and tills that had been overridden by glaciers [*Sauer et al.*, 1990; *Sauer and Christiansen*, 1988]. Pleistocene meltwater has also been preserved in shallow bedrock aquifers by overlying confining units, such as lake bed clays and clay-rich tills (shown in Figure 3), which prevented flushing by more recent recharge.

[11] While fluxes of fresh groundwater to oceans are probably volumetrically insignificant [*Zekster et al.*, 1973], interest has grown as hydrologists have recognized the importance of submarine groundwater discharge as a conveyor of nutrients and pollutants to oceans and estuaries and their implications for marine ecology and biogeochemistry [*Kohout*, 1966; *Li et al.*, 1999; *Slomp and Cappellen*, 2004]. Sea level declines can increase the hydraulic gradients between the continents and the oceans. It is likely that during sea level lowstands, higher chemical fluxes to the global oceans occurred. These temporal changes may be important to earth scientists attempting to estimate long-term chemical fluxes (of carbon and nitrogen) to the oceans. If nutrient fluxes during glacial maxima are significantly larger than today, then modern flux estimates may significantly underestimate nutrient fluxes to the global ocean on geologic timescales.

2. GEOCHEMICAL AND ISOTOPIC TRACERS FOR LAURENTIDE ICE SHEET MELTWATERS

[12] Because with few exceptions [*Bekele et al.*, 2003] fluid pressure anomalies associated with ice sheets seem to have dissipated, elemental and isotope geochemistry provide important constraints on ice sheet–aquifer interactions and paleohydrology. Figure 6 shows a conceptual model of age distribution of paleowaters in a confined aquifer system.

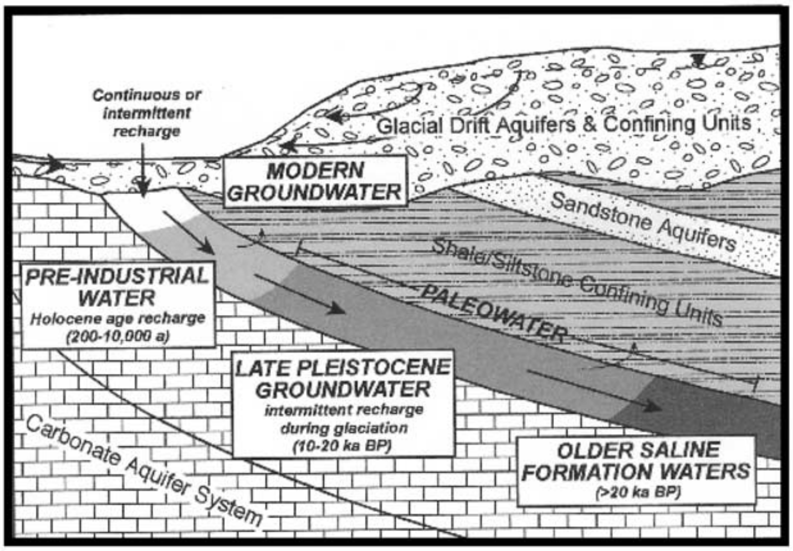

Figure 6. Conceptual model of fluid flow and groundwater age distribution in confined carbonate aquifers along the margins of glaciated sedimentary basins. Flow is assumed to be restricted to the confined aquifer with relatively minor amounts of cross-formational flow. Figure 6 is adapted from *Edmunds* [2001].

For evidence of late Pleistocene recharge to be preserved in groundwater systems, there needs to be a sufficient volume of water with a distinct isotopic signature entering a groundwater system where flow and mixing are small or negligible over long time periods such as 10 to 20 ka [*Loosli et al.*, 1998, *Remenda et al.*, 1994]. Unfortunately, chemical dispersion along the flow path results in the smearing of any high-resolution signal (i.e., abrupt changes in $\delta^{18}O$ values of recharge [*Loosli et al.*, 1998]). In addition, leakage of groundwater across confining units diminishes the possibility of a simple reconstruction of paleoclimatic conditions from confined aquifer systems [*Szabo et al.*, 1997].

2.1. Timing of Meteoric Recharge and Groundwater Residence Times

[13] Carbon 14 is often used for age dating groundwaters that are less than or equal to 30,000 years old, which is within the transition period from the late Pleistocene to Holocene. Several mass balance and theoretical methods have been developed to account for the addition or removal of carbon along flow paths and to estimate the apparent groundwater age (for a review of the various methods see *Clark and Fritz* [1997]). The multiple assumptions required in ^{14}C calculations, and isotopic exchange and dilution of carbon in aquifers, can lead to large errors in the calculated ^{14}C ages of groundwater. Additional tracers (e.g., $\delta^{13}C$ of dissolved inorganic carbon, $^{87}Sr/^{86}Sr$, $\delta^{34}S$ of SO_4^{2-}, noble gases, and elemental chemistry) should be integrated with ^{14}C analyses to better constrain groundwater "ages." It is important to note also that older groundwater in confined aquifers may mix with younger groundwater by diffusion, dispersion, or cross-formational mixing, significantly affecting the age of waters in adjacent aquifers [*Sudicky and Frind*, 1981; *Sanford*, 1997; *Bethke et al.*, 1999; *Bethke and Johnson*, 2002]. This effect is often ignored in groundwater age studies. Thus the piston flow conceptual model (Figure 6) may be too simple to explain the age distribution of groundwater in aquifer systems. Additional isotopic methods not mentioned here, such as ^{36}Cl and ^{86}Kr, may also be employed to determine the age of paleowaters (see, e.g., *Clark and Fritz* [1997] and *Sturchio et al.* [2004] for further discussion).

2.2. Stable Isotope Composition of the Laurentide Ice Sheet

[14] In order to investigate mixing relations of Pleistocene meltwaters, Holocene recharge, and older saline fluids in confined aquifers it is necessary to constrain the isotopic composition of end-member waters. Oxygen and hydrogen isotopes are chemically conservative in low-temperature groundwater systems, making them useful tracers of water sources, mixing relations, and recharge temperatures. The mean annual $\delta^{18}O$ values of modern precipitation in North America range from approximately −2 to −22‰ Vienna standard mean ocean water, dependent on geographic location [*Rozanski et al.*, 1993; *Coplen and Kendall*, 2000; International Atomic Energy Agency/World Meteorological Organization, Global Network of Isotopes in Precipitation (GNIP) database, 1998, available at http://isohis.iaea.org/GNIP.asp]. Estimates of the $\delta^{18}O$ values of the Laurentide Ice Sheet and Pleistocene precipitation have been derived from studies of pore waters in glacial tills and proglacial lake bed clays, groundwater in confined aquifers, wood cellulose, and carbonate-producing organisms. The $\delta^{18}O$ values of Pleistocene-age pore waters in thick (up to 25 m) glacial tills and lake bed clays in southwestern Ontario are 5 to 8‰ lower than present-day precipitation in the region (−9 to −10‰). Relatively slow groundwater flow velocities (<0.05 cm/yr) and low hydraulic gradients in the clay-rich surficial sediments likely prevented rapid flushing of these

paleowaters by more recent recharge [*Desaulniers et al.*, 1981]. *Remenda et al.* [1994] reported $\delta^{18}O$ values as low as −25‰ in pore waters in glacial tills in southern Saskatchewan and northern Ontario; both sites are discussed in detail in section 5. Pleistocene-age waters in underlying Silurian-Devonian carbonate aquifers in the Great Lakes region show a similar depletion in ^{18}O, with $\delta^{18}O$ values ranging from −14.2 to −13.0‰ [*McIntosh and Walter*, 2006]. Stable isotope studies of ancient wood cellulose (9500 to 22,000 years B.P.), from sites across North America, suggest that the average $\delta^{18}O$ value of the Laurentide Ice Sheet was approximately −16.6 to −12‰ [*Yapp and Epstein*, 1977; *Edwards and Fritz*, 1986]. The oxygen isotope composition of benthic ostracodes in the Great Lakes region indicates that lake waters had a $\delta^{18}O$ value of −22 to −17‰ 10,600 to 7600 ^{14}C years B.P. These ^{18}O-depleted surface waters were likely sourced from melting of the Laurentide Ice Sheet [*Rea et al.*, 1994; *Dettman et al.*, 1995]. The low oxygen and hydrogen isotope values of Pleistocene recharge were likely the rule rather than the exception during the past 2 million years. Higher stable isotope values of precipitation, consistent with modern climatic conditions, have occurred since the Holocene. Between 10,000 and 22,000 years before present the average isotopic values of continental precipitation increased.

[15] A few studies have suggested that late Pleistocene climate may have been milder and atmospheric circulation patterns were such that $\delta^{18}O$ and δD values of meteoric waters were possibly closer to modern precipitation values. In commenting on the study of *Weaver and Bahr* [1991], *Siegel et al.* [1992] report $\delta^{18}O$ values up to −9‰ for the late Pleistocene glacial ice lobes from isotopic studies of subglacially precipitated carbonate cements and confined groundwater in the midcontinent region of the United States, similar to modern precipitation [*Siegel*, 1991]. *Ma et al.* [2005] also report relatively high $\delta^{18}O$ and δD values (−8.7 and −56.3‰, respectively) for subglacial meltwaters in Mississippian-age sandstone aquifers in Michigan, possibly caused by changes in atmospheric circulation, relative to modern climatic conditions [*COHMAP Members*, 1988]. Mixing with saline fluids at depth in aquifers can also significantly increase the $\delta^{18}O$ and δD values of groundwaters. In summary, estimated $\delta^{18}O$ values for melting of the Laurentide Ice Sheet range from approximately −25 to −9‰.

2.3. Noble Gas Composition of Subglacial Meltwaters

[16] Noble gas concentrations of subglacial meltwater are expected to be distinct from meteoric recharge or lakes [*Kipfer et al.*, 2002]. In polar ice, noble gases are trapped in the form of air bubbles. In the firn layer (up to ∼100 m thick) the pore structure of the ice is connected. Below this layer, air bubbles are isolated as the pores close off and thus are preserved during downward transport. During basal melting of the ice under high ambient pressures the air bubbles dissolve, and the meltwater is forced into the groundwater system without exposure to the atmosphere. Because of the absence of atmospheric disequilibrium the excess air component of this groundwater should be high. Recently, *Vaikmäe et al.* [2001] reported excess Ne for an Estonian aquifer system that was overrun by the Fennoscandian ice sheet. The Ne levels were 2–5 times above atmospheric saturation levels, which Vaikmäe et al. noted was highly unusual. These groundwaters also had low $\delta^{18}O$ values (−20‰) believed to be derived from ice sheet meltwaters. Studies focusing on the noble gas composition of glacial meltwaters hosted within confined aquifer systems are a promising area of research.

3. EVIDENCE OF ICE SHEET–AQUIFER INTERACTIONS FROM INTRACRATONIC SEDIMENTARY BASINS

[17] Formation waters in sedimentary basins and confined coastal aquifers typically have long residence times (thousands to millions of years) and are usually very saline (35 to >250 g/L total dissolved solids (TDS) [*Hanor*, 1987b]). Pleistocene glaciation exposed regional aquifers along the margins of northern latitude sedimentary basins and within coastal sedimentary sequences by glacial erosion and a drop in sea level, respectively. Recharge of large volumes of dilute waters into saline aquifers profoundly altered their salinity distribution and isotope composition over relatively short geologic timescales (<1 Ma). In sections 3.1–3.8 we review numerous studies that utilize elemental and isotope geochemistry of confined groundwater to evaluate the extent of ice sheet–aquifer interactions.

[18] The majority of paleohydrologic studies of basinal-scale flow systems in North America have focused on the midcontinent region of the United States (Figures 1 and 7). This area is characterized by a number of intracratonic sedimentary basins that were glaciated during the Pleistocene. The Michigan, Illinois, Appalachian, and Forest City basins contain Paleozoic sediments and highly saline formation waters (>250 g/L). Recharge of glacial meltwater beneath the Laurentide Ice Sheet diluted and displaced saline fluids to great depths, significantly modifying the salinity structures and reorganizing groundwater flow patterns. Ice sheet loading was especially important for driving meltwater into regional aquifers in this region, given the low topographic gradients and high-salinity fluids.

3.1. Illinois and Forest City Basins

[19] *Clayton et al.* [1966] first observed low $\delta^{18}O$ and δD values in a few brines in the Illinois and Michigan basins that could not be explained by infiltration of modern precipitation. They suggested that meteoric waters were recharged during the Pleistocene when climatic conditions were colder than the present. In the 1980s and early 1990s, *Siegel* [1989, 1990, 1991, 1992] and *Siegel and Mandle* [1984] systematically studied the isotopic evidence for glacial recharge into the Cambrian-Ordovician aquifer system in the Illinois and Forest City basins. A plume of dilute waters, with less than 500 mg/L TDS, extends from the northwestern margin of the Illinois Basin (i.e., the Hollan-

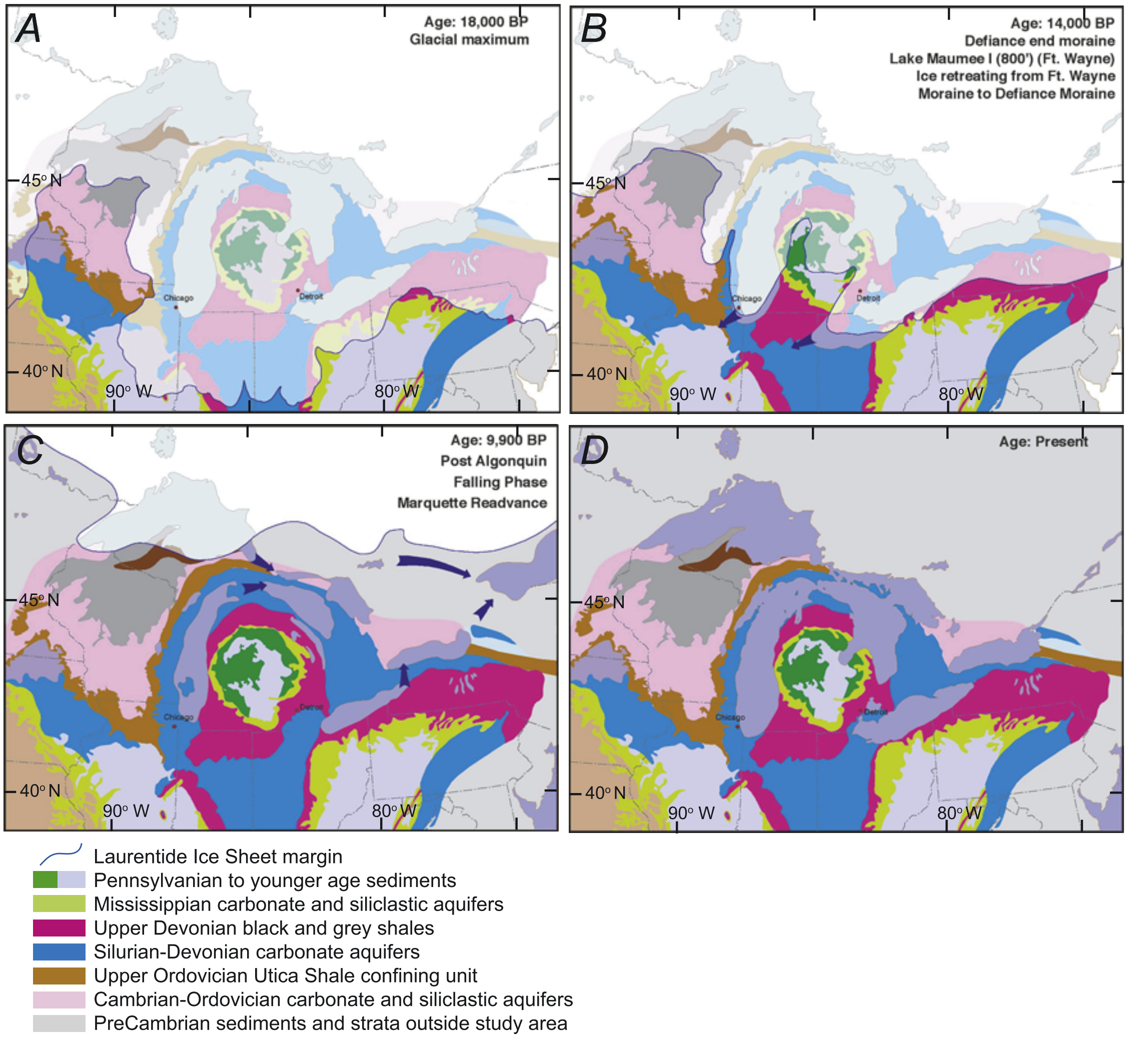

Figure 7. Retreat of the Laurentide Ice Sheet, following the Last Glacial Maximum, in relation to underlying Paleozoic regional aquifer systems and confining units in the Great Lakes region.

dale Embayment) to the south, perpendicular to modern hydraulic gradients (Figure 8). Oxygen isotope values (and correlated δD) of plume waters are -9 to -2‰ lower than modern precipitation in the area and were likely sourced from subglacial recharge. These paleowaters are a principal drinking water source for the densely populated Chicago metropolitan area.

[20] The plume of glacial meltwater in the Cambrian-Ordovician aquifers mixed with basinal brines at depth along the western margin of the Illinois Basin [*Stueber and Walter*, 1994]. Large volumes of glacial meltwater also recharged the overlying Silurian-Devonian carbonate aquifers and migrated to great depths. A lobe of dilute waters (<20 g/L TDS) extends from the northern margin of the basin to $\sim$1 km depth, $\sim$300 km from the carbonate subcrop (Figure 8) [*McIntosh et al.*, 2002]. The north-to-south orientation of the meteoric water lobe is parallel to the axis of the Laurentide Ice Sheet. Confined groundwater in the Silurian-Devonian aquifers has δ^{18}O values as low as -15.3‰, with carbon 14 "ages" ranging from 17 to 50 ka B.P. [*Eberts and George*, 2000; *McIntosh and Walter*, 2006]. Formation waters in Silurian-Devonian aquifers down gradient in the Illinois Basin show mixing of glacial meltwater and brines derived from evapoconcentrated seawater; oxygen isotope values range from -8.6 to 1.8‰ [*Stueber and Walter*, 1991; *McIntosh et al.*, 2002]. Fine-grained sediments, such as shales and siltstones, separate the major aquifer systems. The relatively dilute waters in the basal Cambrian-Ordovician and Silurian-Devonian aquifers show no signs of cross-formational mixing with overlying higher-salinity fluids in Mississippian-Pennsylvanian aquifers.

[21] Within the Cambrian-age Mount Simon aquifer in the Hollandale Embayment of southeastern Minnesota, there is strong evidence that aquifer–ice sheet interactions have had a profound influence on temporal variations in recharge. Histogram analysis of the ^{14}C data originally presented by *Lively et al.* [1993] suggests that there is little evidence of groundwater recharge between 12 and 14 ka, the widely accepted timing of the last glacial advance of the Des Moines lobe in this region [*Patterson*, 1998]. Because of the extensive sampling density along the flow path reported by *Lively et al.* [1993], it is unlikely that the absence of 12–14 ka groundwater is due to inadequate

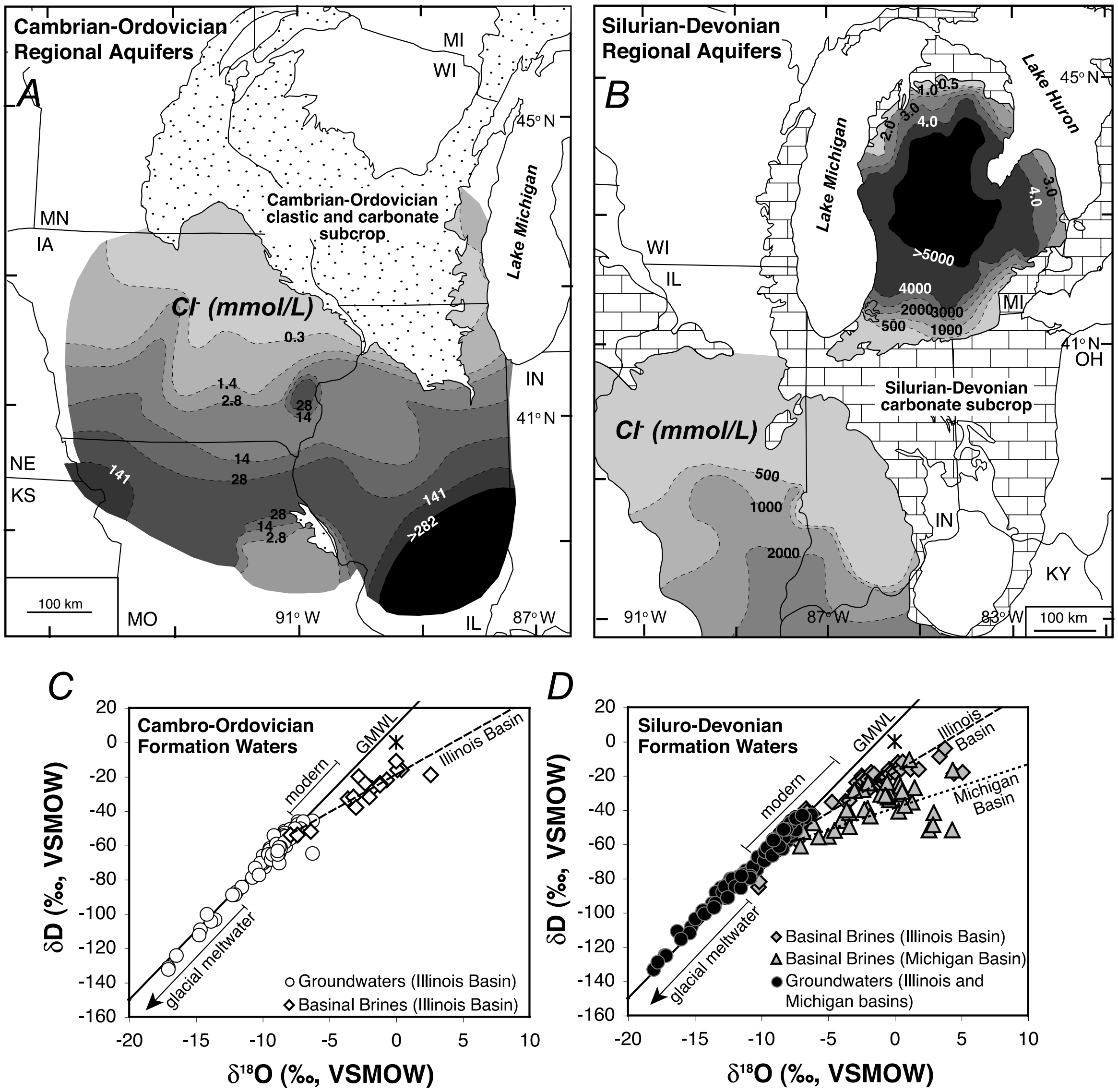

Figure 8. Geochemical and isotopic evidence of glacial recharge into Paleozoic basinal-scale aquifer systems, midcontinent region, United States. (a) Cl- content of formation waters in Cambrian-Ordovician aquifers in the Illinois and Forest City basins. (b) Cl- content of formation waters in Silurian-Devonian aquifers in the Illinois and Michigan basins. Note the difference in Cl- contours between Figures 8a and 8b. Oxygen and hydrogen isotope composition of formation waters in (c) Cambrian-Ordovician and (d) Silurian-Devonian aquifers within the Illinois, Michigan, and Forest City basins. The isotopic value for standard mean ocean water (SMOW) is shown by the star, and the solid line represents the global meteoric water line (GMWL) [*Craig*, 1961]. Figure 8 is modified from *Siegel* [1989], and *McIntosh and Walter* [2006].

sampling. We postulate that the absence of recharge in this area was due to the presence of permafrost features beyond the Des Moines lobe terminus.

3.2. Michigan Basin

[22] Paleozoic aquifers, such as the Cambrian-Ordovician and Silurian-Devonian systems, are extensive in the glaciated midcontinent region and were likely pathways for meltwater into other basins, such as the Michigan and Appalachian basins. Silurian-Devonian aquifers along the eastern margin of the Michigan Basin are confined by thick clay-rich tills (Figure 8). Isotopic studies of pore water in the glacial tills indicate they are Pleistocene in age and have not been flushed out by more recent recharge, as mentioned in section 2.2 [*Desaulniers et al.*, 1981]. Oxygen isotope values of shallow groundwater in underlying Devonian shales and carbonates are exceptionally low (−17.5 to −16‰), compared to modern recharge (−11 to −9‰) [*Husain et al.*, 1998]. Pleistocene meltwater mixed with brines in deeper Devonian strata [*McNutt et al.*, 1987; *Weaver et al.*, 1995]. Groundwater in Silurian-Devonian carbonate aquifers, along the northern margin of the Mich-

igan Basin, also have low $\delta^{18}O$ and δD values, ranging from -15.0 to -10.4‰ and -103.4 to -74.5‰, respectively [*McIntosh and Walter*, 2006]. These paleowaters (carbon 14 "ages" from ~12 to 24 ka) are located beneath lake bed clays along the shallow basin margin and downdip in the Michigan Basin beneath the Upper Devonian shales.

[23] Pleistocene glaciation also affected confined groundwater in Mississippian to Pennsylvanian-age sediments in the Michigan Basin. Loading of the Port Huron lobe of the Laurentide Ice Sheet, in the Saginaw Bay lowlands area of the Michigan Basin, drove meltwater into basinal aquifers and reversed current hydrologic gradients [*Hoaglund et al.*, 2004]. Meltwater mixed with saline fluids at depth in the Saginaw Formation (Pennsylvanian age). The ^{18}O- and ^{2}H-depleted brines ($\delta^{18}O$ values as low as -18.5‰ and Cl > 600 mg/L TDS) are now refluxing into the Saginaw Bay lowlands and Lake Huron [*Kolak et al.*, 1999]. Pleistocene-age waters (up to ~17 ka B.P.) have also been detected in the Marshall Sandstone aquifer system (Mississippian age) in the central Michigan Basin [*Ma et al.*, 2004].

3.3. Appalachian Basin

[24] Groundwater in the Silurian Lockport dolomite, in western New York (Appalachian Basin), shows evidence of glacial meltwater intrusion with $\delta^{18}O$ values (-13.5‰) similar to estimates for the Wisconsin Ice Sheet (-20 to -16‰) and/or proglacial Lake Tonawanda (-13.5 to -11‰), which covered the carbonate escarpment [*Bartos et al.*, 2000]. This glacial meltwater may have dedolomitized the aquifer matrix, significantly altering the formation water chemistry and host mineralogy. Dedolomitization of carbonate aquifers by glacial meltwater was also observed along the northern margin of the Michigan Basin [*McIntosh and Walter*, 2006].

3.4. Pleistocene Glaciation Linked to Generation of Microbial Gas in Fractured Black Shales

[25] Recharge of glacial meltwater into Silurian-Devonian carbonate aquifers, along the margins of the Michigan and Illinois basins, has economic significance, as this meltwater migrated into overlying fractured organic-rich Upper Devonian shales and enhanced generation of microbial methane [*Martini et al.*, 1996, 1998; *McIntosh et al.*, 2002] (Figure 9). Gas production from Upper Devonian fractured shales accounts for a large portion of the United States' total gas production [*Hill and Nelson*, 2000]. Glaciation likely promoted microbial methanogenesis by significantly diluting the salinity of ambient formation waters and dilating natural fractures. Microbial gas is generated in situ at relatively shallow depths, and CO_2 and CH_4 are adsorbed onto the organic matrix. In contrast, conventional natural gas resources are generated by thermal degradation of organic matter at depth in sedimentary basins over geologic timescales (millions of years), and gases migrate from source rocks to stratigraphic traps. This unique microbial gas resource was generated by CO_2 reduction following Pleistocene glaciation (<18 ka), as shown by the covariance of δD values of shale waters and coproduced CH_4, high alkalinity values (>10 meq/kg), and high $\delta^{13}C_{DIC}$ values (>20‰) [*Martini et al.*, 1996] (Figure 9). The Na-Cl-Br relations and stable isotope content of shale fluids in the areas of high microbial activity show that ambient formation waters were significantly diluted by Pleistocene recharge. High salinities were maintained by freshwater dissolution of halite in evaporite-bearing carbonate aquifers along the flow path into the overlying fractured shale [*McIntosh and Walter*, 2005]. Interestingly, subglacial recharge generated Pleistocene-age NaCl brines along the Michigan Basin margins, which have displaced and are now mixing with older Paleozoic NaCaCl brines at depth.

3.5. Western Canada Sedimentary Basin

[26] The Western Canada Sedimentary Basin (WCSB) is bounded by the Canadian Cordillera to the west and the Canadian Shield to the east (Figure 10). The basin extends from the northern Great Plains of the United States to just below the Arctic Circle (62°N latitude) in Canada. The entire WCSB was glaciated except for regions in the north central United States and the Cypress Hills in southeastern Saskatchewan and southwestern Alberta. The wedge of Paleozoic and Mesozoic sediments in the basin contains two major regional aquifers: the basal Cambrian sandstones and the Devonian through Mississippian carbonates. Thick Mesozoic shales confine the regional aquifers. The basin is divided into two subbasins: the Williston and Alberta basins. The eastern margin of the WCSB was glaciated during the Pleistocene. The hydrogeology of the Alberta Basin has been studied by *Bachu* [1995, 1999]. The paleohydrogeology of the WCSB has been studied from the perspective of long-range oil migration and metallogenesis by *Garven* [1985, 1989] although he did not consider the effects of ice sheet hydrogeology [*Grasby and Chen*, 2005]. *Bekele et al.* [2003] compared the relative importance of glacial unloading and sediment erosion in explaining the occurrence of subhydrostatic pressures within shale units of the Alberta Basin.

[27] Modern groundwater flow in the Williston Basin is topographically driven from recharge areas in the southwest (Black Hills) to discharge areas in the northeast (Manitoba Escarpment, Figures 10a and 10b). During Pleistocene glaciation, however, loading of ice sheets (up to 3 km thick) is believed to have reversed regional-scale groundwater flow and recharged glacial meltwaters to great depths within confined Paleozoic aquifers (Figure 10c) [*Grasby et al.*, 2000]. Figure 10d shows the isotopic evidence for mixing of glacial meltwaters with basinal fluids and modern meteoric recharge. Infiltration of meltwaters into the Devonian carbonate aquifers significantly diluted brines and dissolved large quantities of evaporites (Figure 10e). These ^{18}O-depleted Na-Cl waters are now emerging along the northeastern margin of the basin (Figure 10d). *Grasby and Chen* [2005] observed similar geochemical trends along the glaciated margins of the Alberta Basin. The $\delta^{18}O$ values of brine springs in Manitoba and Alberta are -20 and -25‰, respectively, 6‰ lower than average values for modern precipitation. They found that regions overrun by

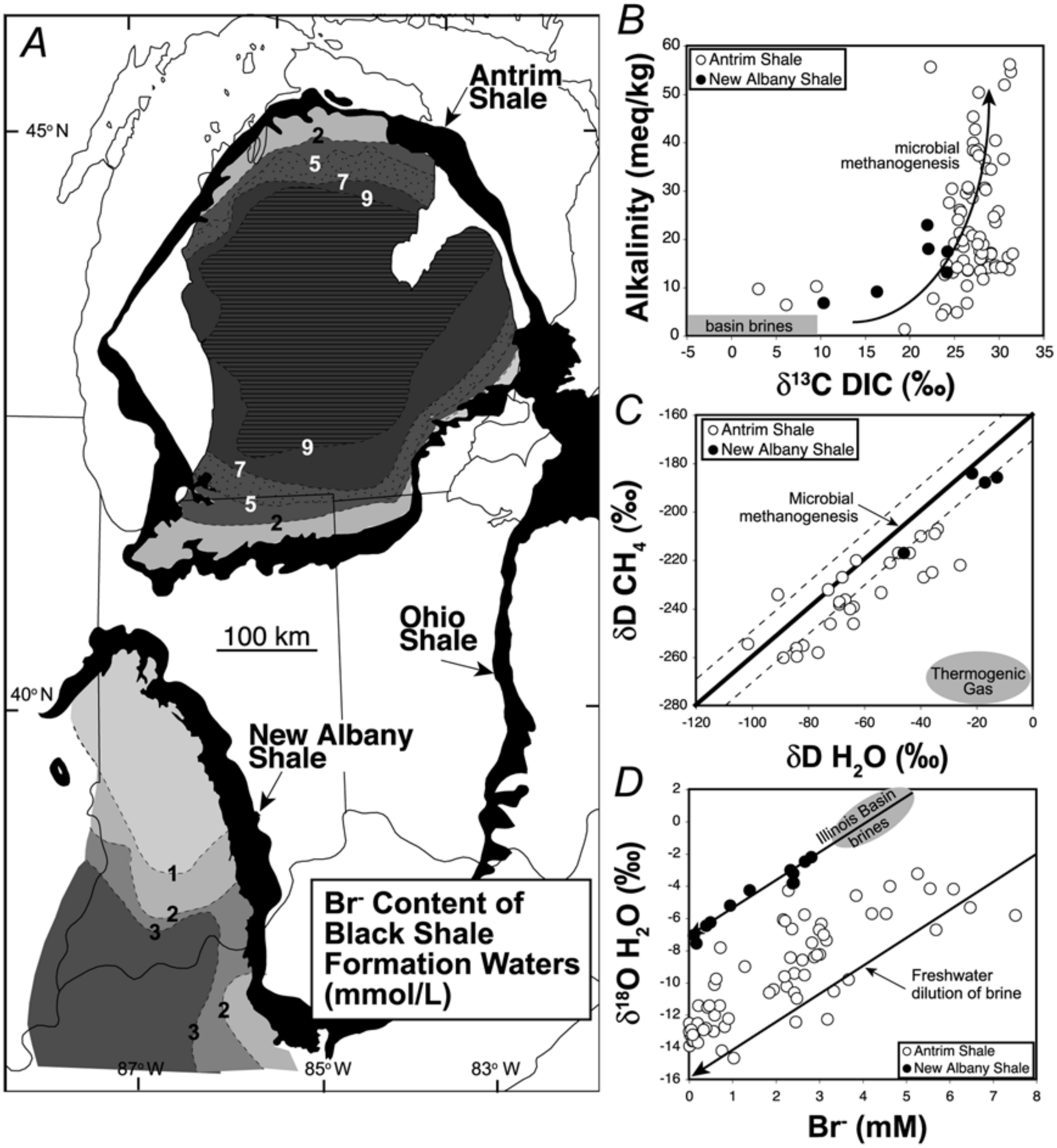

Figure 9. Generation of microbial methane in fractured Upper Devonian organic-rich shales, along the Michigan and Illinois basin margins, following Pleistocene glaciation. (a) Contour map of Br-concentration in shale fluids, showing mixing of dilute meteoric waters with Br-rich basinal brines. (b) Scattergram plot of $\delta^{13}C$ versus alkalinity (dissolved inorganic carbon (DIC)) within shales. Shallow shale formation waters have high alkalinity values and high $\delta^{13}C$ values of DIC, indicative of microbial methanogenesis. (c) Hydrogen isotope values of coproduced shale waters and methane plotted along the equilibrium line for microbial CO_2 reduction [*Schoell*, 1980], shown by the solid line. Methane was produced in situ with the dilute formation waters. (d) Scattergram plot of $\delta^{18}O$ versus bromide for shales. The relatively low $\delta^{18}O$ value of the freshwater end-member suggesting that these meteoric waters were recharged during Pleistocene glaciation. Figure 9 is modified from *Martini et al.* [1996, 1998], *Schoell* [1980], and *McIntosh et al.* [2002].

the Laurentide Ice Sheet along the northeastern margin of the basin were unusually fresh relative to the south. They attributed this to recharge into the outcropping or subcropping of carbonate aquifer systems in this region.

[28] The highly permeable Silurian-Devonian carbonate aquifers were the major avenue for glacial recharge into the Williston and Alberta basins. *Grasby and Chen* [2005] show that the aquifers were able to effectively drain the large volume of glacial meltwaters generated by the Laurentide Ice Sheet. High subglacial pore pressures accumulated in areas underlain by less permeable strata, such as some parts of the Canadian Shield. Esker systems in western Canada are more common in areas underlain by Canadian Shield crystalline rocks and are relatively uncom-

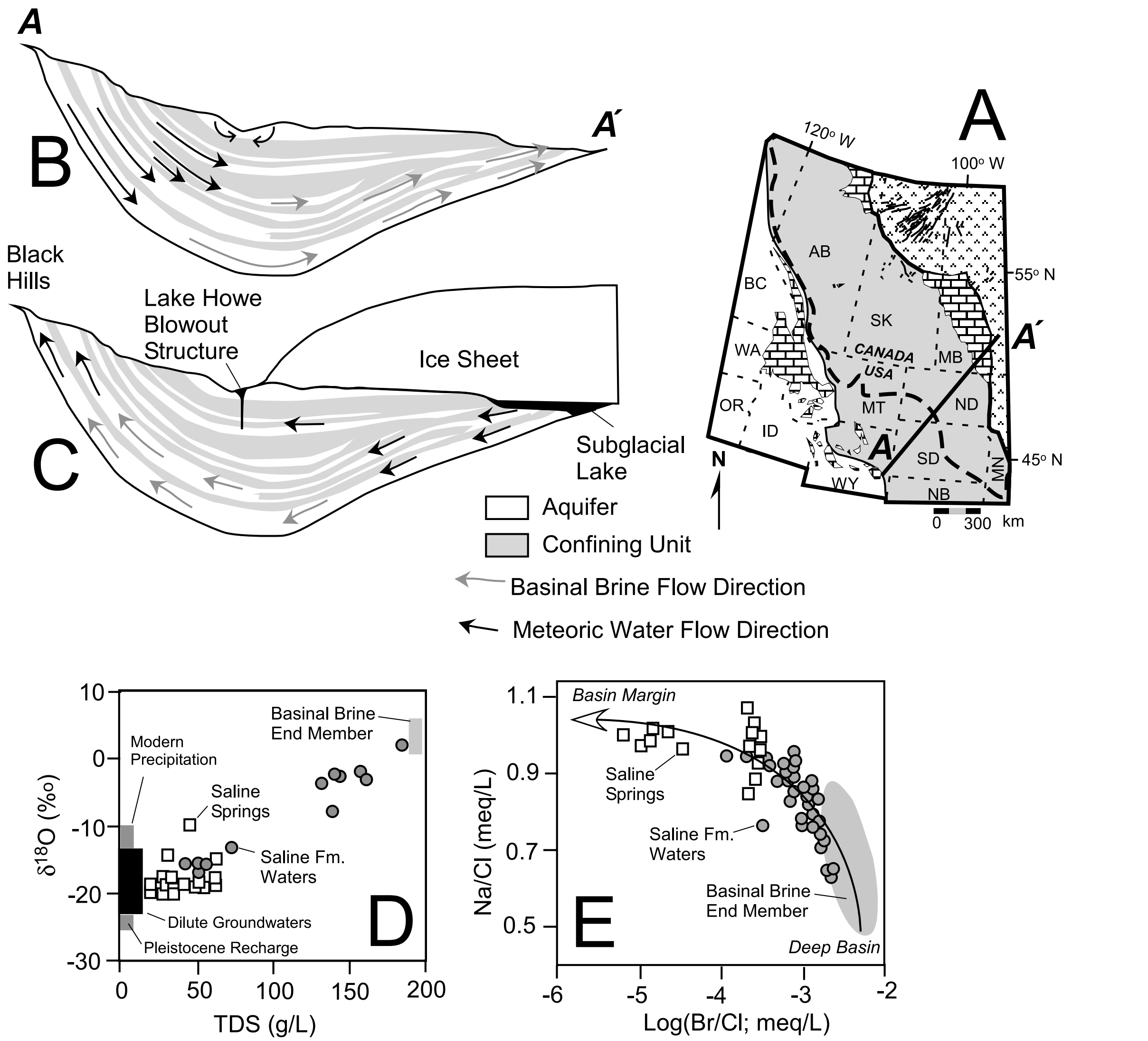

Figure 10. (a) Surface geologic map indicating location of relatively low permeability, Precambrian crystalline bedrock of the Canadian shield (hatched pattern) and Cretaceous shales (shaded pattern) as well as more permeable Paleozoic carbonate aquifer (carbonate pattern) outcrops. The position of esker deposits (thick, sinuous solid line segments) and the location of cross section A-A′ are also shown. Esker deposits are largely confined to low-permeability sediments. (b) Modern versus (c) Pleistocene hydrology in the Williston Basin along cross section A-A′. (d) Oxygen isotope composition of meteoric waters and basinal brines in the Williston Basin, showing mixing of Pleistocene-age recharge and remnant saline fluids. (e) Na-Cl-Br relations of basin formation waters. Glacial meltwaters dissolved halite in Devonian carbonate aquifers, generating waters with high Na/Cl and low Cl/Br ratios. These isotopically depleted, NaCl-rich waters are now refluxing as saline springs along the basin margins. Figure 10 is modified from *Grasby et al.* [2000] and *Grasby and Chen* [2005].

mon south of the shield [*Clark and Walder*, 1994]. The only exception is where the Laurentide Ice Sheet overran the low-permeability shales in the Western Canadian Basin (Figure 10e) [*Grasby and Chen*, 2005].

3.6. Great Plains Aquifer System

[29] The Great Plains Aquifer System, to the south of the WCSB, is one of the largest and most economically important regional aquifers in North America. It extends from north central United States to New Mexico, through vital agricultural regions, and is bordered by the Rocky Mountains to the west. *Gosselin et al.* [2001] detected groundwaters with low δ^{18}O values (-17‰) in the confined portions of the Lower Cretaceous Dakota Sandstone in northeastern Nebraska. They concluded that "cold glacial meltwater" is one of the primary sources of water in the Dakota Aquifer. Regional aquifers in the Great Plains and WCSB are rapidly being depleted to satisfy agricultural and municipal water supply demand. The relatively long residence times of paleowaters in these flow systems have profound implications for water resources, as these high-quality waters cannot be replenished on human timescales.

[30] In their regional study of the Dakota Aquifer and its confining layers, *Bredehoeft et al.* [1983] noted that they were unable to account for the observed pattern of Cl^-

concentrations within the Dakota-Newcastle Aquifer. Although the flow system is from east to west, with discharge occurring along the eastern flank of South Dakota, Cl^- concentrations increase from west to east to a maximum value of about 2000 mg/L in mid state and then decrease eastward to lows of 100 mg/L. As Cl^- is a conservative species at these concentrations, and it is very unlikely that precipitates of Cl^- formed, only dilution is likely to have so dramatically and systematically decreased the Cl^- concentrations. We propose that these data, coupled with isotopic and Cl^- evidence from two samples taken from the northeastern Nebraska part of the Dakota Aquifer [*Gosselin et al.*, 2001], indicate that the Dakota Aquifer was recharged by glacial melt water where it outcrops or subcrops at its eastern boundary. This hypothesis is similar to what *Grasby et al.* [2000] proposed for the late Pleistocene paleohydrology of the Williston Basin. Working in wetlands in the vicinity of the Red River of the North near Grand Forks, North Dakota, *Matheney and Gerla* [1996] found similarly low $\delta^{18}O$ values of −18‰ from wetlands supported by upwelling Dakota Aquifer water, which suggested it was recharged by Pleistocene ice sheet meltwater. Low $\delta^{18}O$ values were also observed at the Manvel site near Grand Forks, North Dakota, where Lake Agassiz clay sits directly on the discharging Dakota Aquifer and has essentially "sampled" this discharge for the past 10 kyr [*Remenda et al.*, 1994].

3.7. Canadian Shield Fractured Bedrock

[31] While fractured bedrock of the Canadian Shield is not usually classified as an aquifer, there is evidence that the Laurentide Ice Sheet has played an important role in modifying fluid chemistry. *Clark et al.* [2000] observed mixing trends between Ca-Na-Cl brines in deep gold mines in the Canadian Shield, which had rock-equilibrated $\delta^{18}O$ values (−10 to −7‰), and ice sheet meltwaters with low $\delta^{18}O$ values (−24‰), relative to modern precipitation in the region (−18.9‰). They suggest that glacial meltwater infiltrated the crystalline bedrock, during times of ice sheet advance and retreat (>10 ka B.P.), and migrated to great depths through fault systems flushing saline fluids. The origin of the anomalous Ca-rich brines in the Canadian Shield is still unknown, although it has recently been attributed to concentration as the result of freezing of seawater beneath Ice Sheets, generating "cryogenic brines" [*Bottomley et al.*, 1999; *Starinsky and Katz*, 2003]. The fact that these brines only occur in high-latitude regions overrun by the Laurentide Ice Sheet gives credence to a cryogenic origin of these saline groundwaters.

3.8. Coastal Aquifers, Eastern Continental Shelf

[32] The Laurentide Ice Sheet advanced out onto the Atlantic continental shelf (dashed lines in Figure 11) forming the islands of Nantucket, Martha's Vineyard, and Cape Cod [*Oldale et al.*, 1978]. Evidence from deep (<1000 m) scientific and petroleum wells drilled in the 1970s indicates that salinity levels in continental shelf aquifers offshore New England are far out of equilibrium with modern sea level conditions. Salinity decreases in continental shelf aquifers in New England observed in boreholes 6001 and 6009 (Figures 11b and 11c and 12a) are likely due to enhanced recharge from beneath the leading edge of the Laurentide Ice sheet. Aquifer salinity levels are less than 5 parts per thousand (ppt) over 100 km offshore of Long Island and New Jersey (well 6009, Figure 11c). In addition, salinity levels within confining units beneath Nantucket Island (see well 6001, Figure 11b) are 30–70% of seawater levels and exhibit a parabolic profile consistent with ongoing vertical diffusion. Analytical models of vertical solute diffusion for the Nantucket confining units suggest that flushing of aquifers beneath Nantucket began in the late Pleistocene as recently as 21 ka assuming a diffusion coefficient of 3.0×10^{-11} m^2/s [*Person et al.*, 2003]. The influx of fresh water into the confined aquifer system may have been facilitated by hydraulic windows in confining units resulting from ice sheet tectonics (Figure 5). Since the recharge area of these confined aquifers is below sea level today in Nantucket Sound, the fresh water beneath Nantucket cannot be due to modern recharge processes. It is also possible that surface water from glacial Lake Nantucket served as an important recharge mechanism [*Marksamer et al.*, 2007].

[33] *Kohout et al.* [1977] proposed that the presence of unusually fresh water within the permeable units of the Atlantic continental shelf could be attributed to meteoric recharge during Pleistocene sea level lowstands. During sea level lowstands, large portions of the continental shelf were exposed to meteoric recharge. Sharp interface models of the freshwater-saltwater distribution on the continental shelf off New Jersey that assumed steady state conditions seemed to confirm this hypothesis [*Meisler et al.*, 1984]. However, numerical models of *Person et al.* [2003], which represented variable-density groundwater flow and solute transport, could not come close to reproducing the low-salinity groundwater observed off Long Island (i.e., the salinity profile in well 6009) by applying boundary conditions consistent with Pleistocene sea level fluctuations (Figures 12b and 12c). These researchers also considered the effects of sub–ice sheet recharge between about 21 and 18 ka when the Laurentide Ice Sheet advanced out onto the continental shelf. Including the effects of ice sheet recharge (i.e., applying a specified head boundary condition for 2000 years equal to 90% of the ice sheet height across much of Long Island) helped to drive the freshwater-saltwater interface much farther out onto the continental shelf (Figures 12d and 12e). Observed salinity conditions were most closely matched by also allowing groundwater to discharge from Miocene/Pliocene aquifers along submarine canyons near the continental slope (Figures 12f and 12g). Simulated recharge induced by Laurentide Ice Sheet meltwater was short-lived (<2000 years) but, on average, about 2–10 times greater than modern subaerial levels.

4. ESTIMATE OF VOLUME OF LAURENTIDE ICE SHEET MELTWATER HOSTED IN NORTH AMERICAN SEDIMENTARY BASINS

[34] We have estimated the volume of Laurentide Ice Sheet meltwater hosted in select aquifer systems across

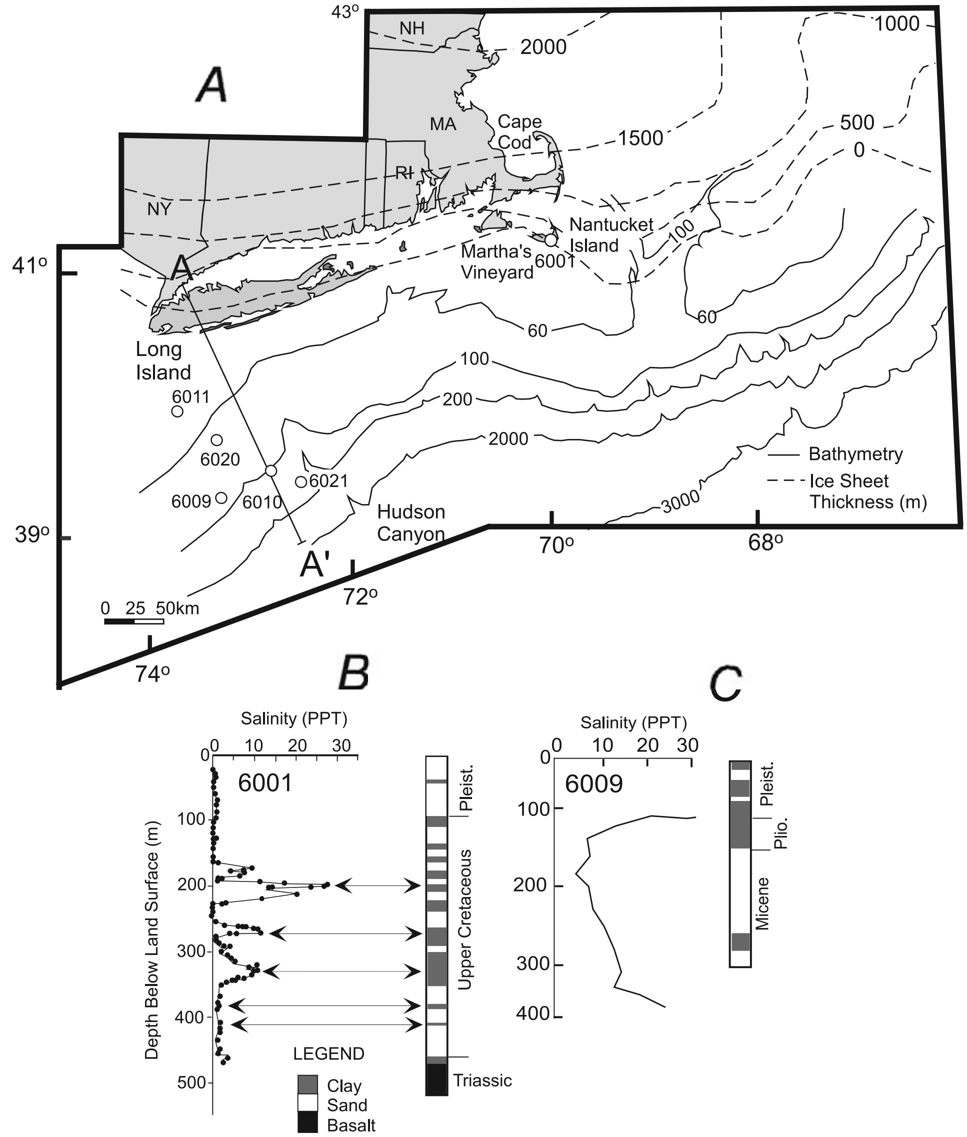

Figure 11. (a) Bathymetric map (solid contour lines in meters) of the Atlantic continental shelf, New England. The dashed contours are maximum reconstructed Laurentide Ice Sheet thickness (in meters) for 21 ka. Location of Amcor wells drilled on the continental shelf is also presented along with associated salinity profiles. Salinity-depth profiles for wells (b) 6001 beneath Nantucket Island and (c) 6009 100 km offshore Long Island and New Jersey. Figure 11 is modified from *Denton and Hughes* [1981], *Hathaway et al.* [1979], and *Person et al.* [2003].

North America using salinity and stable isotope patterns presented from prior studies (Table 1). We estimated the volume of ice sheet recharge by multiplying the areal extent of freshwater emplacement by the combined thickness of formations hosting the meltwater. The areal extent of ice sheet recharge was estimated based on salinity and/or stable isotope data. This must be viewed only as an order of magnitude estimate because of uncertainty in aquifer thicknesses, porosity variations, and groundwater age. In addition, subsequent Holocene recharge, which is assumed to be much smaller, was lumped into this analysis. We found that the total amount of meltwater hosted in these basins totaled 3.7×10^4 km^3 (Table 1). This is not volumetrically significant; it only represents 0.19% of the volume of water stored in the Laurentide Ice Sheet. However, our estimate does not consider glacial meltwater hosted in shallow bedrock aquifers across North America. *Lemieux et al.* [2006] and *Lemieux* [2006] estimated the total amount of recharge from beneath the Laurentide Ice Sheet in Canada using a continental-scale hydrologic model. These authors found that between 5 and 10% of glacial meltwater generated by their code infiltrated into subsurface aquifers over the past 120 ka. The discrepancy between these two estimates can be attributed to differences in the assumptions on which they are based. Our geochemically based estimates only considered ice sheet recharge at the margins of the Laurentide Ice Sheet during Late Wisconsinian and perhaps Illinoian times. This represents a relatively short

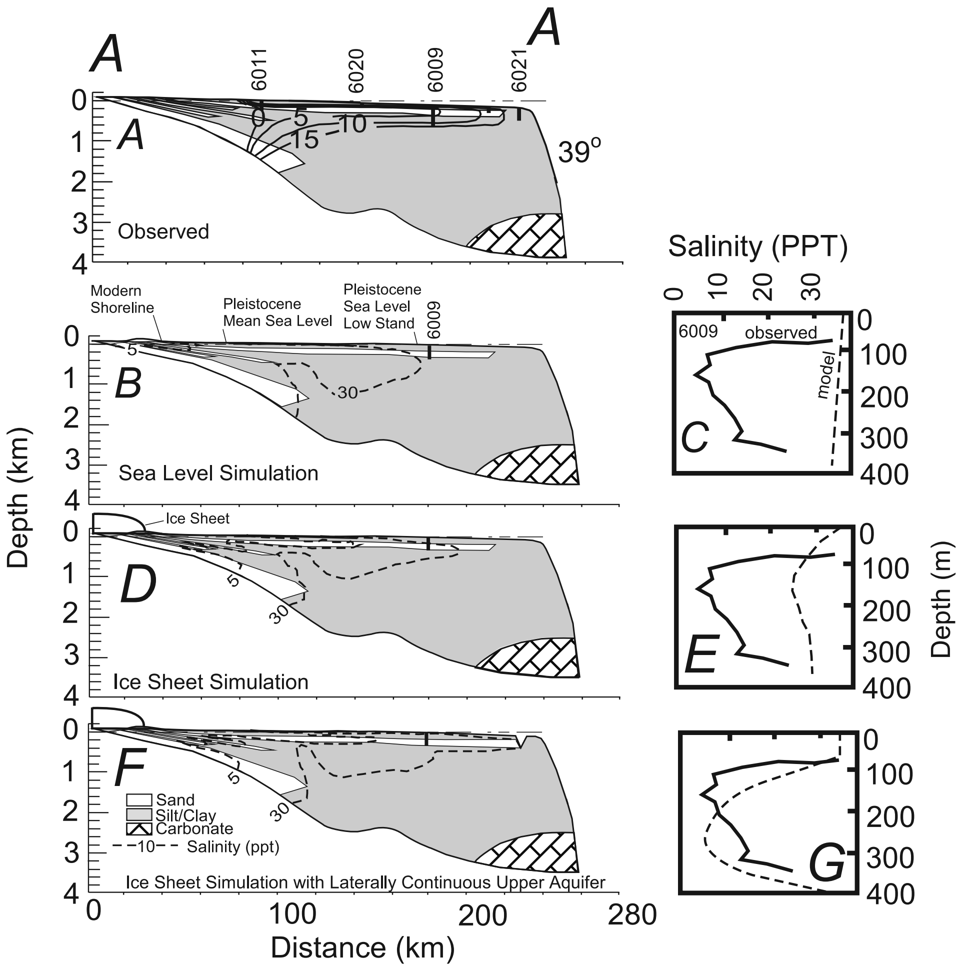

Figure 12. (a) Contour map of salinity patterns (solid lines in parts per thousand (ppt)) for the Atlantic continental shelf sediments offshore Long Island, New York. Contours are inferred from salinity profiles in Amcor wells projected onto the section. The location of the cross section is shown in Figure 11a. (b) Computed salinity contours (dashed lines, ppt) are after 10 sea level cycles about Pleistocene mean level (40 m below modern) using a period of 100,000 years with an amplitude of 120 m. (c) Comparison of computed (dashed) and observed (solid) salinity verses depth profiles for well 6009 after 10 sea level cycles. (d) Computed salinity contour maps for the Atlantic continental shelf sediments offshore Long Island, New York, representing ice sheet recharge. (e) Comparison of computed (dashed) and observed (solid) salinity verses depth profiles for well 6009 representing ice sheet recharge. (f) Computed salinity patterns assuming ice sheet loading but with end of aquifer exposed to continental shelf along marine canyon. Ice sheet simulations are presented following 2000 years of imposed ice sheet boundary conditions. (g) Comparison of computed (dashed) and observed (solid) salinity verses depth profiles for well 6009 assuming ice sheet loading but with end of aquifer exposed to continental shelf along marine canyon. Figure 12 is modified from *Person et al.* [2003].

period of time. *Lemieux et al.* [2006] model results are based on integrated recharge across all of Canada over the Wisconsinian time period. Thus it is not surprising that their estimates are larger. If we only consider infiltration of sub–ice sheet meltwater during the last glacial maximum (10,000 years at a rate of about 2.0×10^{10} m^3/yr), then the *Lemieux et al.* [2006] estimate is only about a factor of 4 greater than our results (2.0×10^5 km^3).

[35] The study by *Grasby et al.* [2000] documents the longest-distance infiltration event of glacial meltwater (~300 km) into clastic and carbonate aquifers [*Bachu and Hitchon*, 1996]. Assuming an ice sheet head of 3000 m, aquifer porosity of 0.1, and an ice sheet infiltration event that lasted 2000 years, we can estimate the effective hydraulic conductivity of the aquifer system using a form of Darcy's law combined with the definition of velocity (i.e., $v = \Delta x/\Delta t = q/\phi$, where q is the Darcy flux). Substituting Darcy's law and solving for hydraulic conductivity yields $K = \Delta x^2\phi/(\Delta t\Delta h)$, where v is groundwater velocity, ϕ is porosity, h is hydraulic head, Δx is transport distance, Δt is the transport time, and K is hydraulic conductivity. Using this expression and the data from *Grasby et al.* [2000], we find that the effective hydraulic conductivity is about 3.0×10^{-4} m/s. This is at the very high

TABLE 1. Estimate of Volumetric Recharge of Laurentide Ice Sheet Meltwaters in Confined Aquifers of North America

Basin	Area, km^2	Total Aquifer Thickness, m	Porosity	Volume, km^3
Forest City[a]	2.36×10^5	390	0.2	1.8×10^4
Williston[b]	9.0×10^4	900	0.1	8.1×10^3
Michigan[c]	3.7×10^4	800	0.2	5.9×10^3
Illinois[c]	1.9×10^4	800	0.2	3.0×10^3
Atlantic Shelf[d]	2.8×10^4	200	0.3	1.7×10^3

[a]Jordan, St. Peter, and Praire de Chien aquifers [*Siegel*, 1991].
[b]Devonian and Basal aquifers [*Grasby et al.*, 2000].
[c]Silurian-Devonian aquifers [*McIntosh and Walter*, 2005].
[d]Plio-Pleistocene aquifers [*Person et al.*, 2003].

end of aquifer conductivity and suggests that hydrofracturing may have taken place during the infiltration event.

5. ISOTOPIC AND GEOMECHANICAL/GEOTECHNICAL EVIDENCE FOR ICE SHEET–AQUIFER INTERACTIONS IN CONFINING UNITS

[36] There are two ways that confining units (usually clays and clayey tills) can record evidence of ice sheet interactions:

[37] 1. Stable isotope data from pore water in isolated, very low flow zones within aquitards is one. This evidence relies on deposits from most recent glaciation [i.e., *Hendry and Wassenaar*, 1999; *Remenda et al.*, 1994; *Desaulniers et al.*, 1981]. These data are useful archives of the aggregate $\delta^{18}O$ and δD values for glacial meltwater.

[38] 2. Large-scale deformation within a till sheet or sheets, which includes stratigraphic and properties anomalies and which relies on a detailed and widespread stratigraphic framework in which to place the anomalies (e.g., thrust structures), also provides evidence.

5.1. Aquitard Pore Water as an Archive of Glacial Meltwater

[39] Under conditions of hydraulic isolation, pore water in aquitards deposited or altered in the late Pleistocene may preserve evidence of glacial meltwater. Such aquitards must be sufficiently thick, generally 25 m or greater, unweathered and unfractured for most of their thickness (and thus have a low bulk hydraulic conductivity, usually 5×10^{-11} m/s or lower), have a low hydraulic gradient, and be diffusion-controlled rather than advection-controlled systems (e.g., Figure 13). At depths where these aquitards are hydraulically isolated, it would be expected that pore water chemistry is dilute and that the isotopic value of oxygen and hydrogen isotopes is very low, reflecting the water in which they were deposited. Following glaciation, solute transport is dominated by diffusion producing bell-shaped oxygen isotope profiles (Figure 13c). Within the last 2 decades

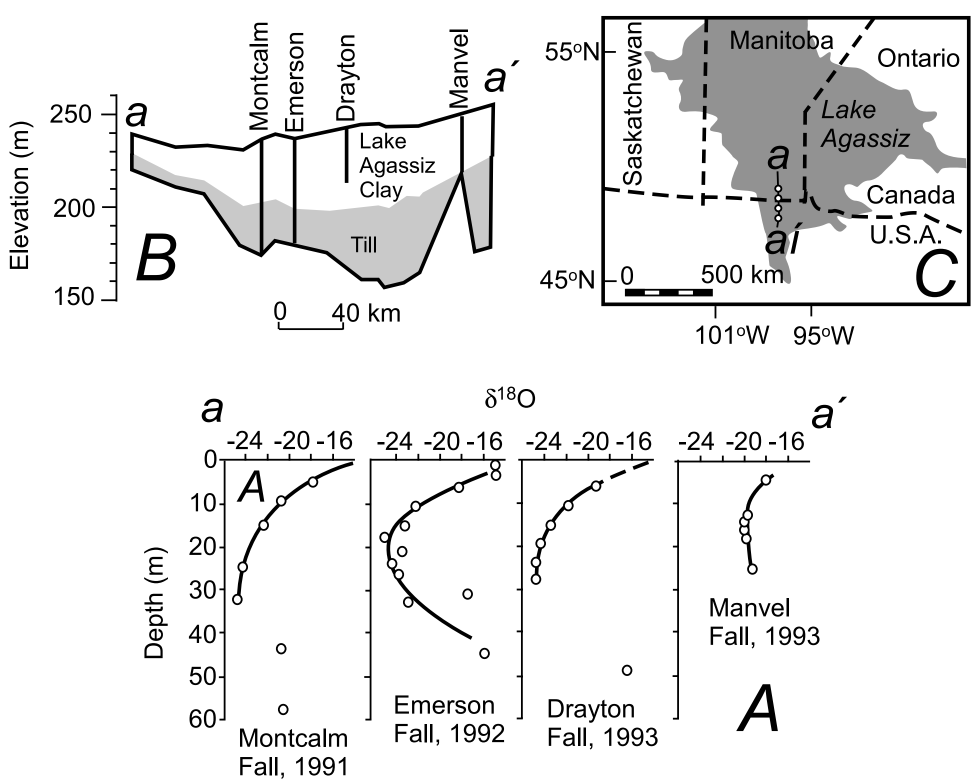

Figure 13. (a) Oxygen isotope profiles from glaciolacustrine deposits from glacial Lake Agassiz in Manitoba, Canada, and Minnesota, United States, along cross section a-a′. (b) Geologic cross section indicating well locations for Figure 13a. (c) Plane view indicating location of glacial Lake Agassiz and position of cross section a-a′. Figure 13 is modified from *Remenda et al.* [1994]. Reprinted with permission, copyright 1994, American Association for the Advancement Science (http://www.sciencemag.org).

several studies of aquitards meeting these criteria have reported $\delta^{18}O$ (or δD) values measured on samples of aquitard pore water that are significantly lower than values for modern precipitation [*Desaulniers et al.*, 1981; *Desaulniers*, 1986; *Remenda et al.*, 1994; *Husain et al.*, 1998; *Hendry and Wassenaar*, 1999]. Early studies by *Desaulniers et al.* [1981] working in clayey tills in the Sarnia region of southwestern Ontario (43°N) reported $\delta^{18}O$ values in groundwater of −15 to −18‰. *Remenda et al.* [1994] found that three of the four sites located in the thick offshore sediments deposited in glacial Lake Agassiz met the criteria for hydraulic isolation and contained water at depth with $\delta^{18}O$ values of −24.5‰. *Remenda et al.* [1994] also reported similar observations from two additional field sites ($\delta^{18}O$ values between −24 and −25‰), located 2000 km apart, a till near Birsay in southern Saskatchewan (50°N) and at a deposit of Lake Barlow-Ojibway clay near New Liskeard in northern Ontario (48°N).

[40] On the basis of ^{2}H-depleted waters at depth and geotechnical data from the King site (50°N), *Shaw and Hendry* [1998] and *Hendry and Wassenaar* [1999] concluded that the aquitard under investigation had been deposited much later than originally thought, about 20 ka versus 38 ka or greater, and thus the pore waters represent connate glacial meltwater. These observations support the idea that −24 to −25‰ represents an average oxygen isotope composition for melting glacial ice at the end of the late Pleistocene, probably for dates of ~11,000 calendar years and earlier, north of about 48°N latitude.

[41] The work of *Buhay and Betcher* [1998] on both pore water and cellulose oxygen isotopes from a 7 m core retrieved from under Lake Winnipeg (53°N) argued for a water more enriched in ^{18}O ($\delta^{18}O$ values from −7 to −9‰) for Lake Agassiz at its later stages. However, the core samples used for this study, obtained from a unit lying below Lake Winnipeg, may not have been hydraulically and isotopically isolated from the overlying lake water and therefore probably do not meet the criteria above. On the basis of different $\delta^{18}O$ values for cellulose (−18.8 to −15.8‰ $\delta^{18}O$) versus deep pore water (−24.4‰ $\delta^{18}O$, consistent with *Remenda et al.* [1994] for the same site) they argued that the relatively high cellulose $\delta^{18}O$ values represents warm, near-surface waters of the epilimnon, while the lower $\delta^{18}O$ values represent the cold, dense, sediment-laden nonevaporated glacial meltwater.

5.2. Stratigraphic and Properties Anomalies

[42] In order to identify anomalies in confining units it is critical that there be a detailed stratigraphic framework from which to work. In addition, as deformation is more likely in unlithified clayey deposits, the tills and Cretaceous shales of Saskatchewan are likely places to find such anomalies. The work of *Christiansen* [1968, 1992] in Saskatchewan identified separate till sheets on the basis of stratigraphic position, carbonate content, Atterberg limits (including natural water contents, liquid limits, and plastic limits), preconsolidation pressures, and presence or absence of staining. This enabled recognition of features such as the Howe Lake Blowout [*Christiansen et al.*, 1982] and Fire Lake Depression [*Christiansen and Sauer*, 1998] to be identified as anomalous. Similar anomalies have undoubtedly been reported elsewhere, but the focus here is on those found in Saskatchewan.

[43] Nonlithified, clayey deposits retain a memory of past loading, including having been overridden by continental ice sheets [*Sauer et al.*, 1990]. Deposits that have compacted under their own weight, such as recent lake clays, are referred to as being normally consolidated. As they undergo self-compaction, their water content decreases as density increases under normal loading. When such deposits have been loaded by ice sheets, they undergo a further decrease in water content and increase in density. When these materials are subsequently unloaded, they do not "rebound" and are referred to as being overconsolidated. Thus clayey deposits that have been overridden by glaciers are considered to be overconsolidated, and they can be tested in the laboratory to determine their preconsolidation load or the load they were once subjected to. In addition, samples can be tested for Atterberg limits. In general, normally consolidated clays will have natural water contents that lie between the plastic limit and the liquid limit. Overconsolidated clays have a natural water content that is less than the plastic limit. However, if overconsolidated clays are subjected to shear, they dilate and soften and return to a state that is somewhat more consolidated than normal and somewhat less consolidated than overconsolidated. In other words, the natural water content increases above the plastic limit, but a memory of the preconsolidation pressure is maintained.

[44] *Christiansen and Sauer* [1998] determined that Fire Lake, a 9 km long, 5 km wide, and 100 m deep depression located in southwestern Saskatchewan, was formed by glacial erosion and shearing of the underlying bedrock composed of unlithified Cretaceous sands, silts, and clays. Beneath the depression the remaining bedrock material was found to be slickensided, folded, brecciated, gouged, and softened. The softening of dense, overconsolidated bedrock, subjected to shear, is consistent with the observations of *Bishop and Henkel* [1953] for the London Clay. They observed that during the expansion of the London underground, excavation caused shearing of the London Clay, which had been heavily overconsolidated by overriding glaciers. In response to the shearing, and in the presence of groundwater, the London Clay changed state, dilated in the presence of water, and became soft.

[45] The discovery of resoftening of overconsolidated London clay by *Bishop and Henkel* [1953] forms the basis for examining the presence of softened zones in Cretaceous shales and clay-rich tills. In particular, softened or disturbed zones within or above otherwise hard, overconsolidated, and competent material have been observed in clays and clayey tills in Edmonton, Alberta (about 54°N) [*Thomson et al.*, 1982], Saskatchewan [*Christiansen and Sauer*, 1998; *Sauer and Christiansen*, 1988; *Sauer et al.*, 1990], and Ontario [*Mirza*, 1983]. *Sauer et al.* [1990] proposed that softened zones observed in southwestern Saskatchewan

from about 49.5° to 54° north latitude in the usually hard, dense, low-water-content Cretaceous clays of the Bearpaw and Lea Park formations in southern Saskatchewan were caused by shearing due to glacial overriding. However, Sauer and coworkers did not address the source of the water taken on during softening.

6. COUPLED MECHANICAL AND THERMAL PROCESSES BENEATH ICE SHEETS

[46] Fluid flow beneath and beyond an ice sheet requires consideration of coupled hydrologic, mechanical, and thermal processes [*Cutler et al.*, 2000; *Boulton and Caban*, 1995; *Lemieux et al.*, 2006; *Bense and Person*, 2006]. Permafrost formation near the toe and terminus of the ice sheet acts as a barrier to groundwater flow, promoting high heads in the ice-free areas, lowering the effective stress, and promoting blowout structures and ice sheet tectonics. Hydrofracturing can modify the permeability of aquifer and aquitard materials. This, in turn, can change the flow patterns lowering fluid pressures. In sections 6.1–6.3 we discuss these processes and the governing equations used to represent them. The governing equations are solved numerically in an attempt to illustrate the consequences of ice sheet–aquifer interactions on groundwater flow patterns.

6.1. Heat Transfer

[47] Permafrost can develop in shallow sediments where the mean annual temperature is at or below zero [*Lunardini*, 1981]. Permafrost can also develop near the toe of an advancing ice sheet. Initial steady state thermal models of *Mooers* [1990] suggest that the permafrost zone would only be a few kilometers wide beyond the ice sheet margin. *Cutler et al.* [2000] found that transient quantitative reconstructions of ice sheet dynamics and heat transfer representing the advance of the Green Bay lobe of the Laurentide Ice Sheet across Wisconsin, United States, suggest that the permafrost width can exceed 100 km. However, this wide swath of permafrost does not last for more than a few thousand years. The governing equation describing conductive heat transfer with phase changes used by Cutler et al. is

$$\left[(c\rho)_b + L\frac{\partial \theta_i}{\partial T}\right]\frac{\partial T}{\partial t} = \nabla_x[\lambda \nabla_x T], \tag{1}$$

where T is temperature, ∇_x is the gradient operator, $(c\rho)_b$ is the bulk heat capacity of the porous media, L_f is the volumetric latent heat of fusion; θ_i and θ_f are the ice and liquid water content, respectively, of the sediment. The changes in enthalpy associated with freezing are represented by the second term on the left-hand side of equation (1), while the first term accounts for time-dependent changes in enthalpy due to temperature changes. The latent heat of freezing term only is applied when the temperature of the bulk sediments approaches zero and can be several orders of magnitude larger than the first term. *Cutler et al.* [2000] used a one-dimensional (vertical) form of equation (1) and did not consider the effects of convective heat transfer on permafrost formation, which is probably appropriate. The bulk heat capacity is the weighted average of the different fluid and solid phases:

$$(c\rho)_b = c_i\rho_i\theta_i + c_f\rho_f\theta_f + c_s\rho_s(1-\phi), \tag{2}$$

where c_i, c_f, and c_s are the specific heat capacity of ice, liquid, and sediments, respectively; θ_i, θ_f, and θ_s are the water content of ice, liquid, and sediments, respectively. In a similar manner the bulk thermal conductivity is given by [*Cutler et al.*, 2000]:

$$\lambda = \lambda_s^{1-\phi}\lambda_f^{\theta_f}\lambda_i^{\theta_i}, \tag{3}$$

where λ_s, λ_f, and λ_i are the thermal conductivity of the sediment, liquid, and ice, respectively. Representative values of the parameters listed in equations (1)–(3) can be found in Table 2.

[48] Boundary and initial conditions needed to solve equation (1) are problematic because they depend on thermal conditions at the base of the ice sheet. This, in turn, is controlled by both conductive and convective heat transfer within the glacier, latitude-dependent temperatures along the ice sheet surface, and melting due to frictional heating. These combined effects result in vertical temperature gradients typically about 10°C/km through the ice sheet, which is about a third of the background geothermal gradient (30°C/km) in the lithosphere. If the temperature at the base of the ice sheet exceeds the pressure melting temperature, a liquid water phase will exist. *Boulton et al.* [1995] notes that this water can move along as thin films in tunnels or channels or through sediments and fractured crystalline rock if permeability is sufficiently high. The presence of liquid water under high pressure at the base of active ice sheets is documented in numerous recent publications focusing on ice sheet dynamics of Antarctica [e.g., *Engelhard and Kamb*, 1997].

6.2. Groundwater Flow

[49] To date, most studies that have developed quantitative models of groundwater flow beneath ice sheets have utilized static representations of ice sheet geometry and neglected the effects of hydromechanical loading (last term on right-hand side of equation (4) [e.g., *Boulton et al.*, 1995; *Piotrowski*, 1997; *Person et al.*, 2003]. If the ice sheet overrides low-permeability sediments, then the effects of ice sheet loading ($d\eta/dt$ in equation (4)) need to be represented [*Lerche et al.*, 1997; *Bekele et al.*, 2003; *Lemieux et al.*, 2006]. The governing groundwater flow equation appropriate for ice sheet loading is

$$\nabla_x[\mathbf{K}\nabla_x(h)] = S_s\left[\frac{\partial h}{\partial t} - \frac{\rho_{\text{ice}}}{\rho_f}\frac{\partial \eta}{\partial t}\right], \tag{4}$$

where t is time, ∇_x is the gradient operator, $\mathbf{K}$ is the hydraulic conductivity tensor, h is hydraulic head, ρ_{ice} is ice density, ρ_f is the fluid density, η is the elevation of the top of the ice sheet, and S_s is the specific storage. Representative

TABLE 2. Representative Rock Properties Used in Permafrost and Hydraulic Calculations

Variable	Symbol	Value/Units
Porosity of sediment	ϕ	0.3
Thermal conductivity of fluid	λ_f	0.58 (W m)/°C
Thermal conductivity of sediment	λ_s	2.5 (W m)/°C
Thermal conductivity of ice	λ_i	(W m)/°C
Heat capacity of fluid phase	c_f	4180 J/kg
Heat capacity of sediment	c_s	800 J/kg
Heat capacity of ice	c_i	J/kg
Latent heat of fusion (ice/water)	L	3.03×10^8 J/m^3
Hydraulic conductivity of sediments	K	10^{-4} to 10^{-15} m/s
Specific storage of sediments	S_s	10^{-4} to 10^{-7} 1/m

ranges of hydraulic conductivity and specific storage for aquifers/confining units are presented in Table 2. High values of $\mathbf{K}$ and low values of S_s are representative of permeable sands, while low values of $\mathbf{K}$ and high values of S_s are representative of confining units. If the ice sheet is frozen at its base, then the ice sheet will act as a mechanical load that is capable of generating excess pressures within low-permeability confining units during ice sheet advance and generating underpressures in tight shales during and after rapid periods of deglaciation [*Bekele et al.*, 2003]. The peak load will occur near the ice sheet toe because of the parabolic nature of the ice sheet topography.

[50] Most prior studies have typically assumed no-flow boundary conditions for the base and sides of the sedimentary basin although it is clear that some glacial meltwaters do penetrate into bedrock (see section 3.7). Many prior studies have applied a specified head boundary condition along the top boundary assuming that the head is equal to 90% the local ice sheet elevation because of fluid-ice density differences [*Boulton et al.*, 1995; *Person et al.*, 2003]:

$$h_{\mathrm{bc}}(x) = 0.9\eta(x), \tag{5}$$

where h_{bc} is the value of the specified head and η is the height of the ice sheet. If the sediments are sufficiently permeable, then the fluids would be drained and equation (5) would be inappropriate. Other studies [e.g., *Breemer et al.*, 2002] have specified a recharge condition beneath the ice sheet taking the flux equal to the basal melting rate ($\sim$6 mm/yr). The use of basal melting rates to constrain the amount of infiltration neglects the possibility of routing meltwater through channel networks at the base of the ice sheet. If permafrost exists at the base of an ice sheet, then a specified head equal to the elevation of the land surface is most appropriate for the land surface. The permeability of the permafrost zone should be reduced.

[51] The presence of basinal brines could greatly modify flow patterns that result from ice sheet loading. Fluid density can significantly affect the depth of meltwater penetration. This would require solving a solute transport equation as well. This was considered first by *Person et al.* [2003] along the Atlantic continental shelf where ice sheet meltwater invaded seawater-filled aquifers. Recently, *McIntosh et al.* [2006] and *Lemieux et al.* [2006] considered the effects of variable-density flow due to the presence of subsurface brines during glaciation. In general, the presence of brines restricted subsurface flow to shallow depths. To date, only one study has considered the effects of ice sheet loading [*Van Der Veen*, 1997] and associated lithosphere flexure on groundwater flow in basins [*Lemieux et al.*, 2006]. Flexural adjustments to the lithosphere typically result in a deflection of the land surface that is equal to about one tenth the ice sheet thickness, although transient effects due to mantle flow can modify the magnitude of both a flexural moat and forebulge [*Peltier*, 1996a, 1996b, 1998]. This would influence the potential energy of the ice sheet and hence subsurface flow patterns.

6.3. Hydromechanical Processes

[52] High fluid pressures associated with sediments beneath the ice sheet can cause low–effective stress conditions promoting sediment failure. This led *Boulton and Caban* [1995] to calculate spatial variations in effective stress during ice sheet loading. Effective stress (σ_e) is defined as

$$\sigma_e = \sigma_v - P \cong d\Big[(1-\phi)\rho_s - \phi\rho_f\Big]g - P, \tag{6}$$

Where g is gravity, P is fluid pressure, σ_v is total vertical stress, d is depth, ϕ is porosity, ρ_f is fluid density, and ρ_s is the sediment density. As pore pressures approach lithostatic levels, effective stress will approach zero, and the sediments will become mechanically unstable. Because permafrost beyond the toe of the ice sheet acts as a shallow aquitard, groundwater beneath the frozen ground is driven out beyond the toe of the ice sheet (Figure 4a). The fluid pressures beneath the permafrost beyond the toe of the glacier reflect the far-field ice sheet hydraulic head causing this region to become mechanically weak. *Boulton and Caban* [1995] calculated conditions under which sediment failure would occur beneath the permafrost zone because of changes in the shear strength of the glacial sediments as a result of changes in effective stress:

$$S = C + \sigma_e \tan\varphi, \tag{7}$$

where C is the shear strength of the sediment under zero confining stress, S is the shear strength of the rock, σ_e is the effective stress, and φ is the internal angle of friction ($\sim$0.3). Their study predicted that beneath and beyond the toe of the ice sheet a zone of hydrofracturing and failure would occur as a result of low–effective stress conditions. This helps explain ubiquitous sediment deformation features observed in glacial tills across North America described in sections 1.4 and 5.2 and illustrated in Figure 5 on the New England continental shelf.

7. SENSITIVITY STUDY

[53] To illustrate the coupled nature of hydromechanical and thermal processes, we present a suite of simulations that investigate ice sheet–aquifer interactions during the advance of an ice sheet over the top of a sedimentary basin.

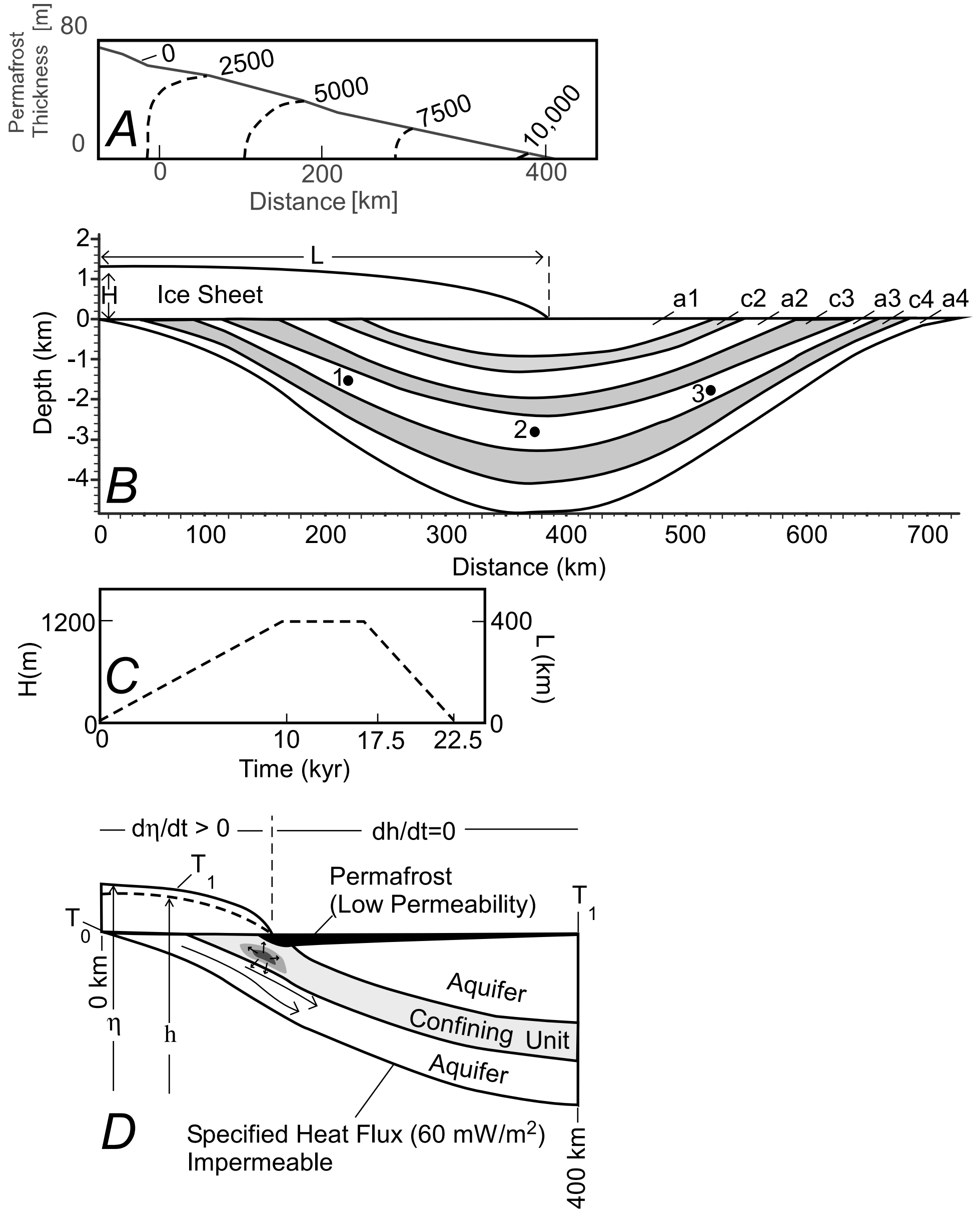

Figure 14. (a) Transient changes in permafrost thickness through time at 0 (solid line), 2500, 5000, 7500, and 10,000 years after the beginning of simulation as the land surface is overrun by the ice sheet. Beneath the ice sheet a basal temperature of 0°C was imposed. (b) Geometry of ice sheet and confined aquifer system used in sensitivity study. The ice sheet thickness (H) and length (L) change with time during the simulation. Numbered bullets denote monitoring points for groundwater flux through time presented in Figure 16. (c) Changes in ice sheet thickness (H) and maximum ice sheet extent (L) through time during simulation. (d) Conceptual model depicting hydrologic and thermal processes and boundary conditions represented by the model. Over the first 400 km the temperatures along the land surface vary from T_o (−1°C) to T_1 (0°C).

We solved the system of equations using the finite element modeling package FlexPDE© (FlexPDE, version 3(10), PDE Solutions Inc., Sunol, California, 2003, available at http://www.pdesolutions.com). Our approach considers the effects of permafrost development and ice sheet loading on groundwater hydrodynamics. Permafrost is represented by using the effective heat capacity following the approach of *Cutler et al.* [2000] (i.e., equations (1)–(3)). In our model we solved a two-dimensional form of equation (1). We decreased the hydraulic conductivity of the frozen sediments by a factor of 1000. This created an effective barrier to groundwater flow. The permafrost waxes and wanes on the basis of changes in the overlying land surface thermal boundary conditions as the ice sheet advances-retreats during the simulation. At the base of the sedimentary pile a heat flux of 60 mW/m^2 was imposed. The sides of the basin were assigned no-flux conditions. Land surface temperature assigned to the top boundary varied between +1° and −1°C from south to north (right to left), respectively. This resulted in a thicker initial permafrost layer growth to the north with

TABLE 3. Hydrologic Properties of Idealized Basin

Unit	K_x, m/s	K_z, m/s	ϕ	S_s, m^{-1}
a1	10^{-6}	10^{-7}	0.2	2×10^{-7}
a2	10^{-6}	10^{-7}	0.2	2×10^{-7}
a3	10^{-6}	10^{-7}	0.2	2×10^{-7}
a4	10^{-7}	10^{-8}	0.2	2×10^{-7}
c1	10^{-10}	10^{-11}	0.4	4×10^{-5}
c2	10^{-10}	10^{-11}	0.4	4×10^{-5}
c3	10^{-10}	10^{-11}	0.4	4×10^{-5}

a maximum thickness of about 80 m (Figure 14a). In the center of the basin the land surface temperature is 0°C, and the permafrost thickness is 0 m. In order to honor changes in ice volume recorded in marine sediment cores, we represented ice sheet advance and retreat in an asymmetric manner (Figure 14c); it takes twice as long for the ice sheet to advance as it does to retreat in our numerical model runs. We considered two end-member conditions for the base of the ice sheet: (1) a temperate glacier with a basal temperature of 0.5°C and (2) a polar glacier with a basal temperature of −1°C. The thickness of the ice sheet was computed using a polynomial expression presented by *Van Der Veen* [1999]:

$$\eta = H\sqrt{\left[\frac{1-x}{L}\right]^2}, \tag{8}$$

where H is ice sheet thickness, L is ice sheet length, x is distance from margin of basin, and η is ice sheet height. The values of H and L were varied linearly through time over a period of 22,500 years (see Figure 14c). For the temperate ice sheet a specified head boundary condition was imposed beneath the ice sheet consistent with equations (5) and (8). No-flow boundary conditions were assumed along the base and sides of the sedimentary pile. A conceptual model illustrating the hydrologic and thermal processes represented in our model is illustrated in Figure 14d. Overpressure generation (bulls eye contour pattern in Figure 14d) can only occur beneath the glacier where $d\eta/dt$ is greater than zero and the sediment permeability is sufficiently low ($<10^{-16}$ m^2).

[54] We chose to represent the aquifer system in a simplified manner. There are four aquifers and three confining units. The permeability of the aquifers and confining units decrease with depth from 10^{-6} to 10^{-7} m^2 and 10^{-10} to 10^{-11} m^2, respectively (Table 3). We did not allow porosity and permeability values to vary with changes in effective stress. The geometry of the sedimentary basin was chosen to resemble an intracratonic sag basin [*Turcotte and Schubert*, 2002] whose margins have been uplifted and where the aquifers and confining units crop out (Figure 14b). There is a gentle slope ($\sim$0.0003) to the water table toward the basin center. The orientation of the basin is north-south. We neglect the effects of fluid density on groundwater flow. Groundwater recharge along the margins of the basin discharges across confining units before discharging in the center of the basin. The maximum groundwater flow rates prior to glaciation within aquifer a3 are relatively low (3.9×10^{-10} m/s).

[55] The simulation was run for 50,000 years to allow all transient effects due to ice sheet loading/unloading and permafrost development to dissipate. Steady state thermal conditions were computed prior to the ice sheet loading in order to determine the permafrost distribution. The distribution of permafrost at the onset of glaciation is shown by the solid line in Figure 14a. Permafrost is thickest at the northern edge of the domain where the land surface temperature is set at −1°C. As the ice sheet advanced over the 10,000 year period, the region of permafrost declined and lagged behind the land surface 0°C position by about 1000 years. The time-dependent nature of permafrost phase change can be observed by the bending of the dashed permafrost thickness lines curving to the right in Figure 14a. If the permafrost melted instantly, these lines would be vertical.

[56] Figure 15 compares computed heads when the ice sheet reached its maximum extent (375 km) and thickness (1200 m) near the center of the basin. For comparison purposes we first show the steady state computed heads using 90% of the ice sheet thickness and assuming no mechanical loading effects (Figure 15a) and a static ice sheet geometry. For the temperate (Figure 15b) and polar (Figure 15c) ice sheet models the computed heads varied distinctly from the steady state model run because of the effects of ice sheet loading and permafrost conditions. As the ice sheet advanced out to its maximum position in the center of the basin, heads within the confining units became overpressured because of the increased overlying ice sheet thickness. For both Figures 15b–15c, heads within the confining unit are higher than in the aquifer beneath the ice sheet when compared to the steady state model results. However, out in front of the ice sheet, heads within the confining unit are low relative to levels within adjacent aquifers when compared to Figure 15a. This is due to slow response time of the confining units. While the magnitude of computed heads varies in all three simulations, the flow system within the aquifers drives groundwater from beneath the ice sheet out to beyond the ice sheet toe. Discharge occurs in a far-field recharge area as well as through the confining unit (i.e., basin-scale flow directions are reversed as suggested by *Grasby et al.* [2000]). For a dry-based ice sheet (i.e., no liquid water present at base of ice sheet, temperature at base of ice sheet below freezing point) overriding the sedimentary basin, the effects of loading are most prominent with vertical leakage occurring out of the confining unit into the adjacent aquifers (Figure 15c). Surprisingly, flow occurs both northward and southward toward the margins of the basin from beneath the center of the ice sheet because of the effects of loading for the polar ice sheet simulation. This is because the compaction-driven flow system is driven by changes in loading rate not because of the thickness of the ice sheet. In general, the maximum overpressure in the confining units lagged behind the position of maximum loading. High excess heads near the land surface on the northern (left) part of the cross section are due to low-permeability conditions associated with permafrost formation.

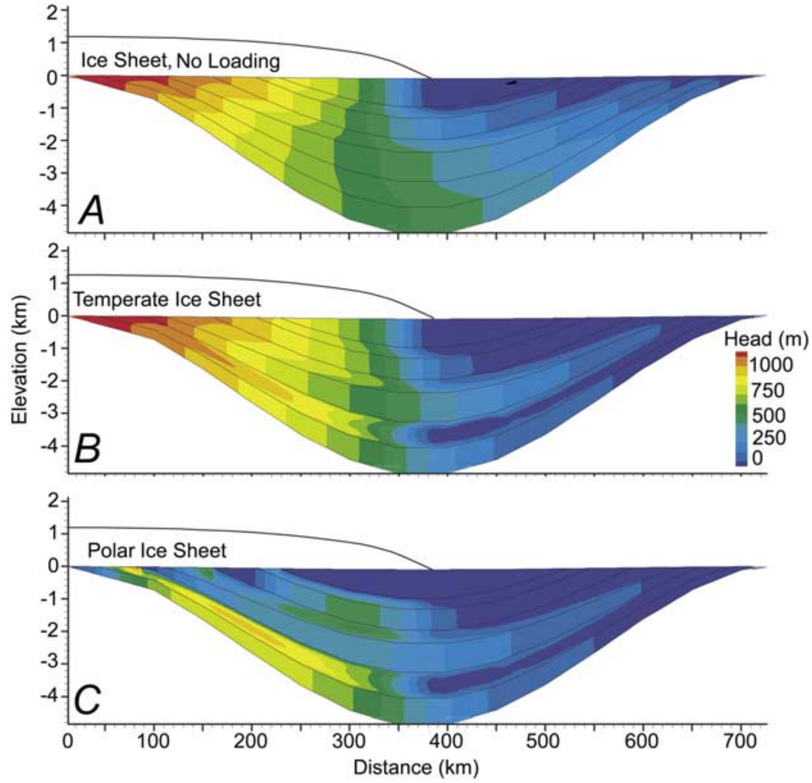

Figure 15. (a) Computed steady state head distribution at the time of maximum ice sheet advance. Along the land surface the imposed specified head boundary condition is equal to 90% the height of the ice sheet beneath the glacier and the elevation of the land surface out in front of the ice sheet. The effects of ice sheet load on heads are not considered in this model. (b) Computed transient head distribution assuming ice sheet loading. The imposed specified head boundary condition is equal to 90% the height of the ice sheet beneath the glacier and the elevation of the land surface out in front of the ice sheet. (c) Computed transient head distribution assuming ice sheet loading. A no-flux boundary condition was imposed beneath the ice sheet and a specified head equal to the elevation of the land surface out in front of the glacier. All computed heads are presented at 10,000 years heads at the time of maximum ice sheet advance.

[57] Figure 16 presents temporal changes in flow rates within the ice sheet at different positions within aquifer a3 during the advance and retreat of the wet-based ice sheet (see Figure 14b for the location of the monitoring points). Flow rates within aquifer a3 ranged from being significantly lower than to higher than steady state lateral flow rates depending on position and timing. Maximum recharge rates recorded in Figure 16 were about 10 times those prior to glaciation. In some instances, groundwater flow patterns reversed direction (lateral flux changes from positive to negative). What is clear is that future attempts to compare computed and observed groundwater tracers such as ^{14}C age dates, environmental isotopic value, or salinity levels will be difficult without incorporating these transient effects (Figure 16).

8. CONCLUSIONS

[58] This paper has shown multiple lines of evidence that indicate that the Laurentide Ice Sheet may have greatly modified groundwater flow patterns within sedimentary basins and altered the isotopic composition and salinity distribution of basinal fluids during Pleistocene ice house conditions. Using salinity and isotopic data, we estimate that about 3.7×10^4 km^3 of ice sheet meltwater has been emplaced in confined aquifers overrun by the Laurentide Ice Sheet; this represents less than 1% of the total water volume

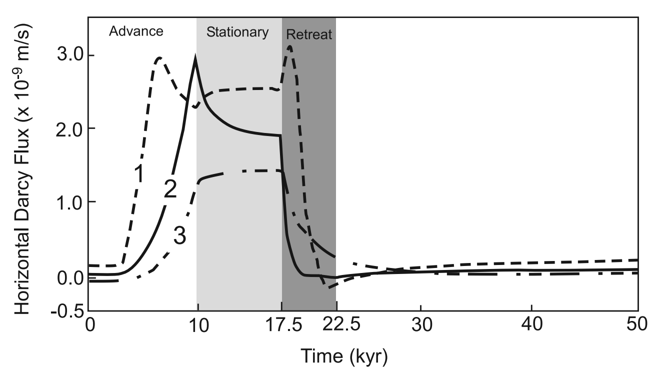

Figure 16. Temporal variations in horizontal groundwater fluxes along aquifer a3 during the advance and retreat of a wet-based glacier over a sedimentary basin. Position of the monitoring points is shown in Figure 14b. Computed fluxes are from the simulation shown in Figure 15b.

of the Laurentide Ice Sheet. Estimates of recharge based on numerical models are considerably higher (5–10% of meltwater generated). If this meltwater recharge does not come into contact with evaporite beds, these groundwaters represent an important water resource. Additionally, the influx of isotopically light, pristine meltwaters may be responsible for enhanced subsurface microbial activity and the formation of commercial methane accumulations in organic-rich sediments (e.g., black shales and coal beds) by significantly diluting ambient formation waters. Drainage of meltwaters beneath the Laurentide Ice Sheet by permeable aquifers would have reduced fluid pressures, would have inhibited the formation of esker deposits, and may have caused ice sheet stagnation [*Grasby and Chen*, 2005]. The circulation of large volumes of ^{18}O-depleted meltwaters within deep confined aquifers makes them useful tracers of groundwater flow velocities, residence times, and regional-scale flow patterns. Future work is needed to integrate environmental isotopic and noble gas tracers to constrain better the timing and volumes of meltwater recharge into confined aquifers. Our study calls into question the notion that groundwater flow patterns were controlled by the configuration of the water table during most of the Pleistocene in areas overrun by the Laurentide Ice Sheet. More complex numerical models are needed to characterize better the hydromechanical and thermal conditions during glaciation. These models should also represent the effects of variable-density flow, solute transport, and the flexural response of the lithosphere to ice sheet loading.

[59] **ACKNOWLEDGMENTS.** We wish to thank Chris Neuzil and Denis Cohen for sharing their insights on hydromechanical processes related to this manuscript. We also thank Dale Austin, Andee Marksammer, and Kyle Brown for their graphical assistance. This research was supported by a grant from the National Science Foundation (EAR-0337634) to Mark Person and the Morton K. and Jane Blaustein Foundation.

[60] The Editor responsible for this paper was Daniel M. Tartakovsky. He thanks technical reviewers Steve Grasby and Martin Appold and one anonymous cross-disciplinary reviewer.

REFERENCES

Aeschbach-Hertig, W., M. Stute, J. F. Clark, R. F. Reuter, and P. Schlosser (2002), A paleotemperature record derived from dissolved noble gases in groundwater of the Aquia Aquifer (Maryland, USA), *Geochim. Cosmochim. Acta*, *66*, 797–817.

Appold, M., and G. Garven (1999), The hydrology of ore formation in the southeast Missouri district: Numerical models of topography-driven fluid flow during the Ouachita orogeny, *Econ. Geol.*, *94*, 913–935.

Bachu, S. (1995), Synthesis and model of formation-water flow, Alberta Basin, Canada, *AAPG Bull.*, *79*, 1159–1178.

Bachu, S. (1999), Flow systems in the Alberta Basin: Patterns, types and driving mechanisms, *Bull. Can. Pet. Geol.*, *47*, 455–474.

Bachu, S., and B. Hitchon (1996), Regional-scale flow of formation waters in the Williston Basin, *AAPG Bull.*, *80*, 248–264.

Baker, V. R. (1997), Megafloods and glaciation, in *Late Glacial and Postglacial Environmental Changes: Quaternary*, *Carboniferous-Permian*, *and Proterozoic*, edited by I. P. Martini, pp. 98–108, Oxford Univ. Press, New York.

Bard, E., B. Hamelin, and R. Fairbanks (1990a), U-Th ages obtained by mass spectrometry in corals from Barbados: Sea level during the past 130,000 years, *Nature*, *346*, 456–458.

Bard, E., B. Hamelin, and R. Fairbanks (1990b), U/Th ages obtained by mass spectrometry in corals from Barbados, *Chem. Geol.*, *84*, 157–158.

Barnhardt, W. A., W. R. Gehrels, D. F. Belknap, and J. T. Kelley (1995), Late Quaternary sea level change in the western Gulf of Maine: Evidence for a migrating glacial forebulge, *Geology*, *23*, 317–320.

Bartos, J. M., Jr., D. I. D. I. Siegel, and R. S. Noll (2000), Evidence for dedolomitization caused by Pleistocene glacial meltwater in a fractured dolomite, *Geol. Soc. Am. Abstr. Programs*, *32*(7), 356.

Bekele, E., B. Rostron, and M. Person (2003), Fluid pressure implications of erosion unloading, basin hydrodynamics and glaciation in the Alberta Basin, western Canada, *J. Geochem. Explor.*, *78–79*, 143–147.

Bense, V., and M. Person (2006), The impact of ice-sheet mechanical loading and permafrost during glacial cycles on fluid flow patterns in inter-cratonic sedimentary basins, paper presented at 2006 Annual Meeting, Geol. Soc. of Am., Philadelphia, Pa.

Bethke, C. M., and T. M. Johnson (2002), Paradox of groundwater age, *Geology*, *30*, 107–110.

Bethke, C. M., and S. Marshak (1990), Brine migration across North America: The plate tectonics of groundwater, *Annu. Rev. Earth Planet. Sci.*, *18*, 287–315.

Bethke, C., X. Zhao, and T. Torgersen (1999), Groundwater flow and the 4He distribution in the Great Artesian Basin of Australia, *J. Geophys. Res.*, *104*, 12,999–13,011.

Bishop, A. W., and D. J. Hankel (1953), Pore pressure changes during shear in two undisturbed clays, paper presented at 3rd International Conference on Soil Mechanics and Foundation Engineering, Zurich, Switzerland.

Bottomley, D. J., A. Katz, L. H. Chan, A. Starinsky, M. Douglas, I. D. Clark, and K. G. Raven (1999), The origin and evolution of Canadian Shield brines: Evaporation or freezing of seawater? New lithium isotope and geochemical evidence from the Slave craton, *Chem. Geol.*, *155*, 295–320.

Boulton, G. S., and P. E. Caban (1995), Groundwater flow beneath ice sheets: part 2—Its impact on glacier tectonic structures and moraine formation, *Quat. Sci. Rev.*, *14*, 563–587.

Boulton, G. S., and S. Zatsepin (2006), A theory of subglacial groundwater structure and flow in areas of modern and ancient glaciation, paper presented at 2006 Annual Meeting, Geol. Soc. of Am., Philadelphia, Pa.

Boulton, G. S., P. E. Caban, and K. Van Gijssel (1995), Groundwater flow beneath ice sheets: part 1—Large scale patterns, *Quat. Sci. Rev.*, *14*, 545–562.

Bredehoeft, J. D., C. E. Neuzil, and P. C. D. Milly (1983), Regional flow in the Dakota Aquifer: A study of the role of confining layers, *U.S. Geol. Surv. Water Supply Pap.*, *W2237*.

Breemer, C. W., P. U. Clark, and R. Haggerty (2002), Modeling the subglacial hydrology of the late Pleistocene Lake Michigan Loge, Laurentide Ice Sheet, *Geol. Soc. Am. Bull.*, *114*, 665–674.

Buhay, W. M., and R. N. Betcher (1998), Paleohydrologic implications of ^{18}O enriched Lake Agassiz water, *J. Paleolimnol.*, *19*, 285–296.

Christiansen, E. A. (1968), Pleistocene stratigraphy of the Saskatoon area, Saskatchewan, Canada, *Can. J. Earth Sci.*, *5*, 1167–1778.

Christiansen, E. A. (1992), Pleistocene stratigraphy of the Saskatoon area, Saskatchewan, Canada: An update, *Can. J. Earth Sci.*, *29*, 1767–1778.

Christiansen, E. A., and E. K. Sauer (1998), Geotechnique of Saskatoon and surrounding area, Saskatchewan, Canada, *Geol. Assoc. Can. Spec. Pap.*, *42*, 117–145.

Christiansen, E. A., D. J. Genzwill, and W. A. Meneley (1982), Howe Lake: A hydrodynamic blowout structure, *Can. J. Earth Sci.*, *19*, 1122–1139.

Clark, I. D., and P. Fritz (1997), *Environmental Isotopes in Hydrogeology*, 328 pp., CRC Press, Boca Raton, Fla.

Clark, I. D., M. Douglas, K. Raven, and D. Bottomley (2000), Recharge and preservation of Laurentide glacial melt water in the Canadian Shield, *Ground Water*, *38*, 735–742.

Clark, P. U., and J. S. Walder (1994), Subglacial drainage, eskers, and deforming beds beneath the Laurentide and Eurasian ice sheets, *Geol. Soc. Am. Bull.*, *106*, 304–314.

Clayton, L., I. Friedman, D. L. Graf, T. K. Mayeda, W. F. Meents, and N. F. Shimp (1966), The origin of saline formation waters: 1. Isotopic composition, *J. Geophys. Res.*, *71*, 3869–3882.

COHMAP Members (1988), Climatic changes of the last 18,000 years: Observations and model simulations, *Science*, *241*, 1043–1052.

Coplen, T. B., and C. Kendall (2000), Stable hydrogen and oxygen isotope ratios for selected sites of the U.S. Geological Survey's NASQAN and benchmark surface-water networks, *U.S. Geol. Surv. Open File Rep.*, *00-160*.

Craig, H. (1961), *Isotopic Variations in Meteoric Waters*, edited by Y. Kitano, 159 pp., Dowden Hutchinson Ross, Inc., Stroudsburg, Pa.

Cutler, P. M., D. R. MacAyeal, D. M. Mickelson, and B. R. Parizek (2000), A numerical investigation of ice-lobe permafrost interaction around the southern Laurentide Ice Sheet, *J. Glaciol.*, *46*, 311–325.

Denton, G. H., and T. J. Hughes (1981), *The Last Great Ice Sheets*, 484 pp., John Wiley, Hoboken, N. J.

Desaulniers, D. E. (1986), Groundwater origin, geochemistry and solute transport in three major glacial clay plains of east-central North America, Ph.D. dissertation, 445 pp., Univ. of Waterloo, Waterloo, Ont., Canada.

Desaulniers, D. E., J. A. Cherry, and P. Fritz (1981), Origin, age and movement of pore water in argillaceous Quaternary deposits at four sites in southwestern Ontario, *J. Hydrol.*, *50*, 231–257.

Dettman, D. L., A. J. Smith, D. K. Rea, T. C. Moore Jr., and K. C. Lohmann (1995), Glacial melt water in Lake Huron during early postglacial time as inferred from single-valve analysis of oxygen isotopes in ostracodes, *Quat. Res.*, *43*, 297–310.

Dingman, S. L. (1994), *Physical Hydrology*, 575 pp., Macmillan, New York.

Eberts, S. M., and L. L. George (2000), Regional ground-water flow and geochemistry in the Midwestern Basins and Arches Aquifer system in parts of Indiana, Ohio, Michigan, and Illinois, *U.S. Geol. Surv. Prof. Pap.*, *P1423–C*.

Edmunds, W. M. (2001), Palaeowaters in European coastal aquifers: The goals and main conclusions of the PALAEAUX Project, in *Palaeowaters in Coastal Europe: Evolution of Groundwater Since the Late Pleistocene*, edited by W. M. Edmunds and C. J. Milne, *Geol. Soc. Spec. Publ.*, *189*, 1–16.

Edwards, T. W. D., and P. Fritz (1986), Assessing meteoric water composition and relative humidity from ^{18}O and ^{2}H in wood cellulose: Paleoclimatic implications for southern Ontario, Canada, *Appl. Geochem.*, *1*, 715–723.

Engelhard, H., and B. Kamb (1997), Basal hydraulic system of a west Antarctic ice stream: Constraints from borehole observations, *J. Glaciol.*, *43*, 207–230.

Essaid, H. I. (1990), A multilayered sharp interface model of coupled freshwater and saltwater flow in coastal systems: Model development and application, *Water Resour. Res.*, *26*, 1431–1454.

Fisher, T. G., and L. D. Taylor (2002), Sedimentary and stratigraphic evidence for subglacial flooding, south-central Michigan, USA, *Quat. Int.*, *90*, 87–115.

Fisher, T. G., L. D. Taylor, and H. M. Jol (2003), Boulder-gravel hummocks and wavy basal till contacts: Products of subglacial melt water flow beneath the Saginaw lobe, south-central Michigan, USA, *Boreas*, *32*, 328–336.

Freeze, R. A., and P. A. Witherspoon (1968), Theoretical analysis of regional ground water flow: 3. Quantitative interpretations, *Water Resour. Res.*, *4*, 581–590.

Garven, G. (1985), The role of regional fluid flow in the genesis of the Pine Point Deposit, Western Canada Sedimentary Basin, *Econ. Geol.*, *80*, 307–324.

Garven, G. (1989), A hydrogeologic model for the formation of the giant oil sands deposits of the Western Canada Sedimentary Basin, *Am. J. Sci.*, *289*, 105–166.

Garven, G., and R. A. Freeze (1984), Theoretical analysis of the role of groundwater flow in the genesis of stratabound ore deposits: 1. Mathematical and numerical model, *Am. J. Sci.*, *284*, 1085–1124.

Gosselin, D. C., F. E. Harvey, and C. D. Frost (2001), Geochemical evolution of ground water in the Great Plains (Dakota) aquifer of Nebraska: Implications for the management of a regional aquifer system, *Ground Water*, *39*, 98–108.

Grasby, S. E., and R. N. Betcher (2002), Regional hydrogeochemistry of the carbonate rock aquifer, southern Manitoba, *Can. J. Earth Sci.*, *39*, 1053–1063.

Grasby, S. E., and Z. Chen (2005), Subglacial recharge into the Western Canada Sedimentary Basin: Impact of Pleistocene glaciation on basin hydrodynamics, *Geol. Soc. Am. Bull.*, *117*, 500–514.

Grasby, S., K. Osadetz, R. Betcher, and F. Render (2000), Reversal of the regional-scale flow system of the Williston Basin in response to Pleistocene glaciation, *Geology*, *28*, 635–638.

Groen, J., J. Velstra, and A. G. C. A. Meesters (2000), Salinization processes in paleowaters in coastal sediments of Suriname: Evidencefrom δ^{37}Cl analysis and diffusion modelling, *J. Hydrol.*, *234*, 1–20.

Hanor, J. S. (1987a), Kilometre-scale thermohaline overturn of pore waters in the Louisiana gulf coast, *Nature*, *327*, 501–503.

Hanor, J. S. (1987b), Origin and migration of subsurface sedimentary brines, *SEPM Short Course*, *21*, 247 pp.

Haq, B. U., J. Hardenbol, and P. R. Vail (1987), Chronology of fluctuating sea levels since the Triassic, *Science*, *235*, 1156–1166.

Hathaway, J. C., C. W. Poag, P. C. Valentine, R. E. Miller, D. M. Schultz, F. T. Manhiem, F. A. Kohout, M. H. Bothner, and D. A. Sangrey (1979), U.S. Geological Survey core drilling on the Atlantic Shelf, 1979, *Science*, *206*, 515–527.

Hendry, M. J., and L. I. Wassenaar (1999), Implications of the distribution of δD in pore waters for groundwater flow and the timing of geologic events in a thick aquitard system, *Water Resour. Res.*, *35*, 1751–1760.

Hill, D. G., and C. R. Nelson (2000), Gas productive fractured shales: An overview and update, *GasTIPS*, *6*, 4–13.

Hoaglund, J. R., III, J. J. Kolak, D. T. Long, and G. J. Larson (2004), Analysis of modern and Pleistocene hydrologic exchange between Saginaw Bay (Lake Huron) and the Saginaw lowlands area, *Geol. Soc. Am. Bull.*, *116*, 3–15.

Husain, M. M., J. A. Cherry, S. K. Frape, and K. J. O'Shea (1998), Hydrogeology of the regional freshwater aquifer Lambton County, southwestern Ontario, paper presented at 36th Annual Conference, Ont. Pet. Inst., London, Ont., Canada.

Kipfer, R., W. Aeschbach-Hertig, F. Peeters, and M. Stute (2002), Noble gases in lakes and ground waters, *Rev. Mineral. Geochem.*, *47*, 615–700.

Kohout, F. A. (1966), Submarine springs: A neglected phenomenon of coastal hydrology, paper presented at Hydrology and Water Resources Development in a Vulnerable Environment Symposium, Cent. Treaty Org., Ankara, Turkey.

Kohout, F. A., J. C. Hathaway, D. W. Folger, M. H. Bothner, E. H. Walker, D. F. Delaney, M. H. Frimpter, E. G. A. Weed, and E. V. C. Rhodehamel (1977), Fresh groundwater stored in aquifers under the continental shelf: Implications from a deep test, Nantucket Island, Massachusetts, *Water Resour. Bull.*, *13*, 373–386.

Kolak, J. J., D. T. Long, J. M. Matty, G. J. Larson, D. F. Sibley, and T. B. Councell (1999), Ground-water, large-lake interactions in Saginaw Bay, Lake Huron: A geochemical and isotopic approach, *Geol. Soc. Am. Bull.*, *111*, 177–188.

Larson, G. J., J. Ehlers, and P. L. Gibbard (2003), Large-scale glaciotectonic deformation in the Great Lakes basin, USA-Canada, *Boreas*, *32*, 370–385.

Lemieux, J.-M. (2006), Impact of the Wisconsinian glaciation on Canadian continental groundwater flow, Ph.D. thesis, Univ. of Waterloo, Waterloo, Ont., Canada.

Lemieux, J.-M., E. A. Sudicky, W. R. Peltier, and L. Tarasov (2006), Coupling glaciations with groundwater flow models: Surface/subsurface interactions over the Canadian landscape during the Wisconsinian glaciation, paper presented at International Ground Water Symposium, Int. Assoc. of Hydrol. Eng. and Res., Toulouse, France.

Lerche, I., Z. Yu, B. Tgorudbakken, and R. O. Thomsent (1997), Ice loading effects in sedimentary basins with reference to the Barents Sea, *Mar. Pet. Geol.*, *14*, 277–338.

Li, L., D. A. Barry, F. Stagnitti, and J. Y. Parlange (1999), Submarine groundwater discharge and associated chemical input to a coastal sea, *Water Resour. Res.*, *35*, 3253–3259.

Licciardi, J. M., J. T. Teller, and P. U. Clark (1999), Freshwater routing by the Laurentide Ice Sheet during the last deglaciation, in *Mechanisms of Global Climate Change at Millennial Time Scales*, *Geophys. Monogr. Ser.*, vol. 112, edited by P. U. Clark, R. S. Webb, and L. D. Keigwin, pp. 177–201, AGU, Washington, D. C.

Lively, R. S., R. Jameson, E. C. Alexander, and G. B. Morey (1993), Radium in the Mt. Simon-Hinkley Aquifer, east-central and southeastern Minnesota, *Inf. Circ. Minn. Geol. Surv.*, *36*.

Loosli, H. H., B. Lehmann, W. Aeschbach-Hertig, R. Kipfer, W. M. Edmunds, L. Eichinger, K. Rozanski, M. Stute, and R. Vaikmae (1998), Tools used to study paleoclimate help in water management, *Eos Trans. AGU*, *79*(47), 576.

Lunardini, V. J. (1981), *Heat Transfer in Cold Climates*, 731 pp., Van Nostrand Reinhold, New York.

Ma, L., M. C. Castro, and C. M. Hall (2004), A late Pleistocene–Holocene noble gas paleotemperature record in southern Michigan, *Geophys. Res. Lett.*, *31*, L23204, doi:10.1029/2004GL021766.

Ma, L., M. C. Castro, C. M. Hall, and L. M. Walter (2005), Cross-formational flow and salinity sources inferred from a combined study of helium concentrations, isotopic ratios, and major elements in the Marshall Aquifer, southern Michigan, *Geochem. Geophys. Geosyst.*, *6*, Q10004, doi:10.1029/2005GC001010.

Marksamer, A. J., M. A. Person, F. D. Day-Lewis, J. W. Lane Jr., D. Cohen, B. Dugan, H. Kooi, and M. Willet (2007), Integrating geophysical, hydrochemical, and hydrologic data to understand the freshwater resources on Nantucket Island, Massachusetts, in *Subsurface Hydrology: Data Integration for Properties and Processes*, *Geophys. Monogr. Ser.*, vol. 171, edited by D. W. Hyndman, F. D. Day-Lewis, and K. Singha, pp. 143–159, AGU, Washington D. C.

Marshall, S. J., and G. K. C. Clarke (1999), Modeling North American freshwater runoff through the last glacial cycle, *Quat. Res.*, *52*, 300–315.

Marshall, S. J., T. S. James, and G. K. C. Clarke (2002), North American ice sheet reconstructions at the Last Glacial Maximum, *Quat. Sci. Rev.*, *21*, 175–192.

Martini, A. M., J. M. Budai, L. M. Walter, and M. Schoell (1996), Microbial generation of economic accumulations of methane within a shallow organic-rich shale, *Nature*, *383*, 155–158.

Martini, A. M., L. M. Walter, J. M. Budai, T. C. W. Ku, C. J. Kaiser, and M. Schoell (1998), Genetic and temporal relations between formation waters and biogenic methane: Upper Devonian Antrim Shale, Michigan Basin, USA, *Geochim. Cosmochim. Acta*, *62*, 1699–1720.

Matheney, R. K., and P. J. Gerla (1996), Environmental isotopic evidence for the origins of ground and surface water in a prairie discharge wetland, *Wetlands*, *16*, 109–120.

McIntosh, J. C., and L. M. Walter (2005), Volumetrically significant recharge of Pleistocene glacial melt waters into epicratonic basins: Constraints imposed by solute mass balances, *Chem. Geol.*, *222*, 292–309.

McIntosh, J. C., and L. M. Walter (2006), Paleowaters in Silurian-Devonian carbonate aquifers: Geochemical evolution of groundwater in the Great Lakes region since the late Pleistocene, *Geochim. Cosmochim. Acta*, *70*, 2454–2479.

McIntosh, J. C., L. M. Walter, and A. M. Martini (2002), Pleistocene recharge to mid-continent basins: Effects on salinity structure and microbial gas generation, *Geochim. Cosmochim. Acta*, *66*, 1681–1700.

McIntosh, J. C., L. M. Walter, and A. M. Martini (2004), Extensive microbial modification of formation water geochemistry: Case study from a midcontinent sedimentary basin, United States, *Geol. Soc. Am. Bull.*, *116*, 743–759.

McIntosh, J. C., G. Garven, and J. S. Hanor (2006), Reorganization of basinal-scale groundwater flow and salinity gradients during Pleistocene glaciation: Hydrologic modeling study of the Michigan Basin, paper presented at Annual Meeting, Geol. Soc. of Am., Philadelphia, Pa.

McNutt, R. H., S. K. Frape, and P. Dollar (1987), A strontium, oxygen and hydrogen isotopic composition of brines, Michigan and Appalachian basins, Ontario and Michigan, *Appl. Geochem.*, *2*, 495–505.

Meisler, H., P. P. Leahy, and L. L. Knobel (1984), Effect of eustatic sea-level changes on saltwater-freshwater in the northern Atlantic coastal plain, *U.S. Geol. Surv. Water Supply Pap.*, *2255*.

Milliman, J. D., and K. O. Emery (1968), Sea-levels during the past 35,000 years, *Science*, *162*, 1121–1123.

Mirza, C. (1983), Soft zones in the glacial till in downtown Edmonton: Discussion, *Can. Geotech. J.*, *20*, 193–194.

Mooers, H. D. (1990), Ice-marginal thrusting of drift and bedrock: Thermal regime, subglacial aquifers, and glacial surges, *Can. J. Earth Sci.*, *27*, 849–862.

Oldale, R. N. (1988), A late Wisconsin marine incursion into Cape Cod Bay, Massachusetts, *Quat. Res.*, *30*, 237–250.

Oldale, R. N., and S. M. Coleman (1990), Evidence against a late Wisconsinan ice shelf in the Gulf of Maine, *Quat. Sci. Rev.*, *9*, 1–13.

Oldale, R. N., and C. J. O'Hara (1984), Glaciotectonic origin of the Massachusetts coastal end moraines and a fluctuating late Wisconsinan ice margin, *Geol. Soc. Am. Bull.*, *95*, 61–74.

Oldale, R. N., P. C. Valentine, T. M. Cronin, E. C. Spiker, B. W. Blackwelder, J. F. Wehmiller, and B. J. Szabo (1978), Stratigraphy, structure, absolute age, and paleontology of the upper Pleistocene deposits at Sankaty Head, Nantucket Island, Massachusetts, *Geology*, *10*, 246–252.

Oldale, R. N., S. M. Coleman, and G. A. Jones (1993), Radiocarbon ages from two submerged strandline features in the western Gulf of Maine and a sea-level curve for the northeastern Massachusetts coastal region, *Quat. Res.*, *40*, 38–45.

Otvos, E. G. (2005), Numerical chronology of Pleistocene coastal plain and valley development: Extensive aggradation during glacial low sea-levels, *Quat. Int.*, *135*, 91–113.

Pardee, J. T. (1942), Unusual currents in glacial Lake Missoula, Montana, *Geol. Soc. Am. Bull.*, *53*, 1569–1599.

Patterson, C. J. (1998), Laurentide glacial landscapes: The role of ice streams, *Geology*, *26*, 643–646.

Peltier, W. R. (1996a), Mantle viscosity and ice-age ice sheet topography, *Science*, *273*, 1359–1364.

Peltier, W. R. (1996b), Global sea level rise and glacial isostatic adjustment: An analysis of data from the east coast of North America, *Geophys. Res. Lett.*, *23*, 717–720.

Peltier, W. R. (1998), Postglacial variations in the level of the sea: Implications for climate dynamics and solid-earth geophysics, *Rev. Geophys.*, *36*, 603–689.

Person, M., B. Dugan, J. B. Swenson, L. Urbano, C. Sttot, J. Taylor, and M. Willett (2003), Pleistocene hydrogeology of the Atlantic continental shelf, New England, *Geol. Soc. Am. Bull.*, *115*, 1324–1343.

Pewe, T. L. (1983), The periglacial environment in North America during Wisconsin time, in *Late-Quaternary Environments of the United States*, edited by S. C. Porter, pp. 157–188, Univ. of Minn. Press, Minneapolis.

Piotrowski, J. (1997), Subglacial hydrology in north-western Germany during the last glaciations: Groundwater flow, tunnel valleys and hydrological cycles, *Quat. Sci. Rev.*, *16*, 169–185.

Rains, B., J. Shaw, R. Skoye, D. Sjogren, and D. Kvill (1993), Late Wisconsin subglacial megaflood paths in Alberta, *Geology*, *21*, 323–326.

Raymo, M. E., D. W. Oppo, and W. Curry (1997), The mid-Pleistocene climate transition: A deep sea isotopic perspective, *Paleoceanography*, *12*, 559–569.

Rea, D. K., T. C. Moore Jr., T. W. Anderson, C. F. M. Lewis, D. M. Dobson, D. L. Dettman, A. J. Smith, and L. A. Mayer (1994), Great Lakes paleohydrology: Complex interplay of glacial melt water, lake levels, and sill depths, *Geology*, *22*, 1059–1062.

Remenda, V. H., J. A. Cherry, and T. W. D. Edwards (1994), Isotopic composition of old ground water from Lake Agassiz: Implications for late Pleistocene climate, *Science*, *266*, 1975–1978.

Rozanski, K., L. Araguás-Araguás, and R. Gonfiantini (1993), Isotopic pattern in modern global precipitation, in *Climatic Change in Continental Isotopic Records*, *Geophys. Monogr. Ser.*, vol. 78, edited by P. K. Swart et al., pp. 1–36, AGU, Washington, D. C.

Sanford, W. E. (1997), Correcting for diffusion in carbon-14 dating of ground water, *Ground Water*, *35*, 357–361.

Sauer, E. K., and E. A. Christiansen (1988), Preconsolidation pressures in intertill glaciolacustrine clay near Blaine Lake, Saskatchewan, *Can. Geotech. J.*, *25*, 831–839.

Sauer, E. K., L. F. Gareau, and E. A. Christiansen (1990), Softening of overconsolidated Cretaceous clays by glacial erosion, *Q. J. Eng. Geol.*, *23*, 307–324.

Schoell, M. (1980), The hydrogen and carbon isotopic composition of methane from natural gases of various origins, *Geochim. Cosmochim. Acta*, *44*, 649–662.

Shackleton, N. J. (1987), Oxygen isotopes, ice volume, and sea level, *Quat. Sci. Rev.*, *6*, 183–197.

Shackleton, N. J., and N. D. Opdyke (1973), Oxygen isotope and paleomagnetic stratigraphy of equatorial Pacific core V28–238: Oxygen isotope temperatures and ice volumes on a 105 year and 106 year scale, *Quat. Res.*, *3*, 39–55.

Shaw, R. J., and M. J. Hendry (1998), Hydrogeology of a thick clay till and Cretaceous clay sequence, Saskatchewan, *Can. Geotech. J.*, *35*, 1041–1052.

Siegel, D. I. (1989), Geochemistry of the Cambrian-Ordovician aquifer system in the northern Midwest, United States, *U.S. Geol. Surv. Prof. Pap.*, *1405-D*.

Siegel, D. I. (1990), Sulfur isotope evidence for regional recharge of saline water during continental glaciation, north-central United States, *Geology*, *18*, 1054–1056.

Siegel, D. I. (1991), Evidence for dilution of deep, confined groundwater by vertical recharge of isotopically heavy Pleistocene water, *Geology*, *19*, 433–436.

Siegel, D. I. (1992), Discussion of "Geochemical evolution of the Cambrian-Ordovician Aquifer, eastern Wisconsin: 1. Major ion and radionuclide distribution," by T. M. Weaver and J. M. Bahr, *Ground Water*, *30*, 273–275.

Siegel, D. I., and R. J. Mandle (1984), Isotopic evidence for glacial melt water recharge to the Cambrian-Ordovician Aquifer, north-central United States, *Quat. Res.*, *22*, 328–335.

Siegel, D. I., E. Muller, D. Pair, R. Noll, and A. Martini (1992), Isotopic evidence from regional ground water and calcite cements that late Wisconsin continental ice lobes were sustained by tropical air masses, *Geol. Soc. Am. Abstr. Programs*, *24*(7), 240.

Slomp, C. P., and P. V. Cappellen (2004), Nutrient inputs to the coastal ocean through submarine groundwater discharge: Controls and potential impact, *J. Hydrol.*, *295*, 64–86.

Starinsky, A., and A. Katz (2003), The formation of natural cryogenic brines, *Geochim. Cosmochim. Acta*, *67*, 1475–1484.

Stewart, I. S., J. Sauber, and J. Rose (2000), Glacio-seismotectonics: Ice sheets, crustal deformation and seismicity, *Quat. Sci. Rev.*, *19*, 1367–1389.

Stott, D. F., and J. D. Aitken (Eds.) (1993), *The Geology of North America*, vol. D-1, *Sedimentary Cover of the Craton in Canada*, Geol. Soc. of Am., Boulder, Colo.

Stueber, A. M., and L. M. Walter (1991), Origin and chemical evolution of formation waters from Silurian-Devonian strata in the Illinois Basin, USA, *Geochim. Cosmochim. Acta*, *55*, 309–325.

Stueber, A. M., and L. M. Walter (1994), Glacial recharge and paleohydrologic flow systems in the Illinois Basin: Evidence from chemistry of Ordovician carbonate (Galena) formation waters, *Geol. Soc. Am. Bull.*, *106*, 1430–1439.

Sturchio, N. C., et al. (2004), One million year old groundwater in the Sahara revealed by krypton-81 and chlorine-36, *Geophys. Res. Lett.*, *31*, L05503, doi:10.1029/2003GL019234.

Stute, M., P. Schlosser, J. F. Clark, and W. S. Broecker (1992), Paleotemperatures in the southwestern United States derived from noble gases in ground water, *Science*, *256*, 1000–1003.

Stute, M., M. Forster, H. Frischkorn, A. Serejo, J. F. Clark, P. Schlosser, W. S. Broecker, and G. Bonani (1995a), Cooling of tropical Brazil (5°C) during the Last Glacial Maximum, *Science*, *269*, 379–383.

Stute, M., J. F. Clark, P. Schlosser, and W. S. Broecker (1995b), A 30,000 yr continental paleotemperature record derived from noble gases dissolved in ground water from the San Juan Basin, New Mexico, *Quat. Res.*, *43*, 209–220.

Sudicky, E. A., and E. O. Frind (1981), Carbon 14 dating of groundwater in confined aquifers: Implications of aquitard diffusion, *Water Resour. Res.*, *17*, 1060–1064.

Szabo, Z., A. A. Pucci Jr., and M. D. Feigenson (1997), Sr-isotopic evidence for leakage of pore water from clay-silt confining units to the Atlantic City 800-foot sand, Atlantic City, New Jersey, *Proc. Ocean Drill. Program Sci. Results*, *150*, 343–354.

Teller, J. T. (1990), Volume and routing of late-glacial runoff from the southern Laurentide Ice Sheet, *Quat. Res.*, *34*, 12–23.

Teller, J. T., and A. E. Kehew (1994), Introduction to the late glacial history of large proglacial lakes and melt water runoff along the Laurentide Ice Sheet, *Quat. Sci. Rev.*, *13*, 795–799.

Thomson, S., R. L. Martin, and Z. Eisenstein (1982), Soft zones in the glacial till in downtown Edmonton, *Can. Geotech. J.*, *19*, 175–180.

Tóth, J. (1962), A theory of groundwater motion in small drainage basins in central Alberta, Canada, *J. Geophys. Res.*, *67*, 4375–4387.

Turcotte, D. L., and G. Schubert (2002), *Geodynamics*, 456 pp., Cambridge Univ. Press, New York.

Uchupi, E., and A. E. Mulligan (2006), Late Pleistocene stratigraphy of upper Cape Cod and Nantucket Sound, Massachusetts, *Mar. Geol.*, *27*, 93–118.

Uchupi, E., and R. Oldale (1994), Spring sapping origin of the enigmatic relict valleys of Cape Cod and Martha's Vineyard and Nantucket Islands, Massachusetts, *Geomorphology*, *9*, 83–95.

Uchupi, E., G. S. Giese, D. G. Aubrey, and D. J. Kim (1996), The late Quaternary construction of Cape Cod, Massachusetts: A reconsideration of the W. M. Davis Model, *Spec. Pap. Geol. Soc. Am.*, *309*, 69 pp.

Uchupi, E., N. Driscoll, R. D. Ballard, and S. T. Bolmer (2001), Drainage of Late Wisconsin glacial lakes and the morphology and late Quaternary stratigraphy of the New Jersey–southern New England continental shelf and slope, *Mar. Geol.*, *172*, 117–145.

Vaikmäe, R., L. Vaullner, P. H. Loosli, P. Bloser, and M. Juillard-Tardent (2001), Paleogroundwater of glacial origin in the Cambrian-Vendian Aquifer of northern Estonia, in paleowaters, *Geol. Soc. Spec. Publ.*, *189*, 17–27.

Van Der Veen, C. J. (1999), *Fundamentals of Glacier Dynamics*, 462 pp., A. A. Balkema, Brookfield, Vt.

Voss, C. I., and J. Andersson (1993), Regional flow in the Baltic Shield during Holocene coastal regression, *Ground Water*, *31*, 989–1006.

Weaver, T. R., and J. M. Bahr (1991), Geochemical evolution in the Cambrian-Ordovician sandstone aquifer eastern Wisconsin, 2, Correlation between flow paths and ground-water chemistry, *Ground Water*, *29*, 510–515.

Weaver, T. R., S. K. Frape, and J. A. Cherry (1995), Recent cross-formational fluid flow and mixing in the shallow Michigan Basin, *Geol. Soc. Am. Bull.*, *107*, 697–707.

Webb, T., III, K. H. Anderson, P. J. Bartlein, and R. S. Webb (1998), Late Quaternary climate change in eastern North America: A comparison of pollen-derived estimates with climate model results, *Quat. Sci. Rev.*, *17*, 587–606.

Weyhenmeyer, C. E., S. J. Burns, H. N. Waber, W. Aeschbach-Hertig, R. Kipfer, H. H. Loosli, and A. Matter (2000), Cool glacial temperatures and changes in moisture source recorded in Oman ground waters, *Science*, *287*, 842–845.

Winter, T. C. (2001), The concept of hydrologic landscapes, *J. Am. Water Resour. Assoc.*, *37*, 335–349.

Yapp, C. J., and S. Epstein (1977), Climatic implications of D/H ratios of meteoric water over North America (9500–22,000 B. P.) as inferred from ancient wood cellulose C-H hydrogen, *Earth Planet. Sci. Lett.*, *34*, 333–350.

Zekster, I., V. A. Ivanov, and A. V. Meskheteli (1973), The problem of direct groundwater discharge to the seas, *J. Hydrol.*, *20*, 1–36.

Zhu, C., R. K. Waddell, I. Star, and M. Ostrander (1998), Responses of ground water in the Black Mesa Basin, northeastern Arizona, to paleoclimatic changes during the late Pleistocene and Holocene, *Geology*, *26*, 127–130.

V. Bense, School of Environmental Sciences, University of East Anglia, Norwich NR4 7TJ, UK.

J. McIntosh, Department of Hydrology and Water Resources, University of Arizona, Tucson, AZ 85721, USA.

M. Person, Department of Geology, Indiana University, Bloomington, IN 47405, USA. (maperson@indiana.edu)

V. H. Remenda, Department of Geological Sciences and Geological Engineering, Queen's University, Miller Hall, Kingston, ON, Canada K7L 3N6.